

## CONTENTS W through Z

---

Melted-reduced Pigeonite, Vermicular Silica, Si-rich Glasses, and Other Impact-smelting Products in the LAR04315 Ureilite <i>P. H. Warren and A. E. Rubin</i> .....	5155
GASP! Gas-associated Spheroidal Precipitates Related to HASP, Found in Anorthositic Apollo 14 Regolith Breccia 14076 <i>P. H. Warren, E. Tonui, and E. D. Young</i> .....	5379
Evidence of Differing Liquid Regimes in Metallic Magmas <i>J. T. Wasson</i> .....	5387
Nebular Fines, Presolar Grains and Collateral Damage During Chondrule Formation <i>J. T. Wasson</i> .....	5343
Sulfide-Metal Nodules in EH3 Chondrites <i>M. K. Weisberg, H. C. Connolly, D. S. Ebel, and M. Kimura</i> .....	5317
Cosmogenic Radionuclides in a Weathered, 2.8 Million Year Old H-Chondrite Found on Top of Frontier Mountain, Antarctica <i>K. C. Welten, K. Nishiizumi, L. Folco, and M. W. Caffee</i> .....	5350
The Complex Exposure History of a Large L6 Chondrite Shower from Oman <i>K. C. Welten, K. Nishiizumi, D. J. Hillegonds, and M. W. Caffee</i> .....	5382
Impact-related Deformation in the Collar Rocks of the Vredefort Dome, South Africa <i>F. Wieland, R. L. Gibson, and W. U. Reimold</i> .....	5018
What are the Consequences if the “SEP” Solar Noble Gas Component Does Not Exist? <i>R. Wieler, A. Grimberg, and V. S. Heber</i> .....	5067
The Effect of Atmospheric Entry Heating on Micrometeorite Volatile Composition <i>R. C. Wilson, V. K. Pearson, I. A. Franchi, I. P. Wright, and I. Gilmour</i> .....	5207
Implications for the Chicxulub Fireball Derived from a Systematic Analysis of Its Deposits <i>A. Wittmann, D. Stöffler, L. Hecht, and T. Kenkmann</i> .....	5078
Stepwise Chemical Dissolution of Carbonaceous Chondrites: Correlations Between Volatile Trace Elements and Major/Minor Mineral Constituent Elements <i>S. F. Wolf</i> .....	5049
Analysis of Residues Resulting from Mafic Silicate Impacts into Aluminium 1100 <i>P. J. Wozniakiewicz, A. Kearsley, M. J. Burchell, M. J. Cole, and P. A. Bland</i> .....	5076
Planetesimal Formation Induced by Photophoresis at the Inner Edge of the Solar Nebula <i>G. Wurm, O. Krauss, and H. Haack</i> .....	5115
High-Pressure Mineral Assemblages in Shock Melt Veins of Suizhou Meteorite <i>X. Xie, M. Chen, and D. Wang</i> .....	5026
Alkaline Copper Oxide Degradation of Insoluble Organic Matter in Carbonaceous Chondrites <i>H. Yabuta, G. D. Cody, and C. M. O’D. Alexander</i> .....	5386

Mineralogical Study of Augite-bearing Lodranite, NWA2235 and Implication for Its Origin <i>A. Yamaguchi, H. Takeda, and M. Kusakabe</i> .....	5202
Temperature Dependence on the Effects of Aqueous Alteration on Mineralogy and Noble Gas Compositions in Carbonaceous Chondrite Ningqiang <i>Y. Yamamoto, T. Nakamura, T. Noguchi, and K. Nagao</i> .....	5337
Evolution of Differentiated Asteroids as Inferred from Cooling Rates of Magmatic Iron Meteorites <i>J. Yang, J. I. Goldstein, and E. R. D. Scott</i> .....	5146
Fractal Dimension Analysis of Hellas Basin: The Martian Impact Crater Might be Ancient Lakes/Seas <i>G. Yangrui</i> .....	5108
Supernova Mixtures Reproducing Isotopic Ratios of Low Density Graphite Grains <i>T. Yoshida</i> .....	5250
O-Isotopic Distribution of Porphyritic and Non-Porphyritic Chondrules in Acfer 214, CH Chondrite <i>M. Yoshitake and H. Yurimoto</i> .....	5174
Possible Heightened Noctilucent Cloud Activity Near Strong Perseid Maxima <i>M. Zalcik and A. A. Mardon</i> .....	5007
Some Applications of the Chondrite Oxygen Mixing Model <i>B. Zanda and R. H. Hewins</i> .....	5383
Coordinated Structure-Isotope Studies of Presolar Hibonites <i>T. J. Zega, R. M. Stroud, L. R. Nittler, and C. M. O'D. Alexander</i> .....	5375
Pairing and Petrogenetic Relationships Among Basaltic Lunar Meteorites from Northwest Africa <i>R. A. Zeigler, R. L. Korotev, B. L. Jolliff, T. E. Bunch, and A. J. Irving</i> .....	5235
Petrographic and Mineralogical Studies of the Lunar Meteorite Dhofar 1180 <i>A. Zhang and W. Hsu</i> .....	5170
Study of Metal Extracted from Tzarev L5 Chondrite by Mössbauer Spectroscopy and Metalography <i>E. V. Zhiganova and M. I. Oshtrakh</i> .....	5100
Si and C Isotopic Ratios in AGB Stars: SiC Grain Data, Models, and the Galactic Evolution of the Si Isotopes <i>E. Zimmer, L. R. Nittler, R. Gallino, A. I. Karakas, M. Lugaro, O. Straniero, and J. C. Lattanzio</i> .....	5144
Fe-isotopic Fractionation in CB Chondrites <i>J. Zipfel and S. Weyer</i> .....	5321

**MELTED-REDUCED PIGEONITE, VERMICULAR SILICA, SI-RICH GLASSES, AND OTHER IMPACT-SMELTING PRODUCTS IN THE LAR04315 UREILITE.**

Paul H. Warren and Alan E. Rubin. Institute of Geophysics, UCLA, Los Angeles, CA 90095, USA.

Our studies indicate that the anomalous LAR04315 ureilite [1] formed by intense shock, including pyroxene-localized shock melting, of an otherwise normal ureilite. The late, post-decompression (post-parent-body disruption?) "smelting" process that affected all ureilites, mainly by reduction of olivine rims [2], primarily affected shock-melted pyroxene in LAR04315.

Later annealing made the final state of the 1-2 mm pyroxenes crystalline, but recovery from shock-melt is indicated by, inter alia, scattered small voids in almost all of the pyroxene [1]. These voids are typically  $40 \times 20 \mu\text{m}$ , but curved and in some cases vermicular. They comprise ~20 vol.% of the space within pyroxene, or 10 vol% of the rock. Isolated patches of little-altered, void-free pyroxene are usually  $\ll 0.1$  mm across. However, one  $0.9 \times 0.7$  mm low-shock pyroxene consists mainly of large  $\sim 100 \times 100 \mu\text{m}$  void-free patches. During cooling, coarse twins developed in pyroxene, probably as the grains transformed from protoenstatite to pigeonite. Pyroxene compositions are unusually diverse, with random, void-rich pyroxenes showing effects of FeO loss (reduction). But the most FeO-rich analyses, all from the  $0.9 \times 0.7$  mm low-shock pyroxene, are tightly clustered in the normal ureilite fashion at  $W_{\text{O}} 10.3$ ,  $mg \sim 81.8$ . Isolated small void-free patches tend to resemble the low-shock remnant in composition. The voids within pyroxene may not be completely empty. In x-ray maps, they show locally higher Ca, Mg and O, and lower C, than empty (crack) voids.

The original 1-2 mm olivines now consist of mosaics of small (usually  $\ll 0.5$  mm), often angular pieces [1], indicating that they were strongly shocked, shattered, and subsequently welded together by (presumably) the same annealing process that recrystallized the pigeonites. Even so, the olivine avoided pervasive reduction. Tiny metal grains are common between olivine subgrains, but amount to only ~1% of the volume within any original olivine; and although subtle differences between subgrains are apparent in BSE images, these differences are difficult to detect quantitatively. The average olivine core composition,  $F_{\text{O}} 81.9$ , is nearly identical in  $mg$  to the intact pigeonite. For comparison, in 12 other  $\sim F_{\text{O}} 82$  ureilites (literature data), olivine-core  $mg$  is lower, but only by  $1.6 \pm 1.0$  mol%, than pigeonite  $mg$ . In some places, clusters of rounded olivine remnants are surrounded by interstitial pyroxene, typically of relatively high-Ca composition.

In some ferroan ureilites, post-decompression reduction of minor interstitial basaltic melt appears to have locally generated Si-Al-rich melts [2]. A similar process resulted in relatively significant proportions of Si-Al-rich glass in LAR04315, and also long (up to  $\sim 100 \times 5 \mu\text{m}$ ) vermicular grains of a silica phase, with typically ~99.0 wt%  $\text{SiO}_2$ , 0.4%  $\text{Al}_2\text{O}_3$  and 0.2% FeO.

The phase oxidized during the smelting of LAR04315 was presumably, as generally assumed for ureilites, solid C. From the extent of reduction of pigeonite, a remarkably high yield of CO/CO<sub>2</sub> gas is implied: ~0.7 wt% of the rock. The rock probably did not remain a totally closed system during the smelting. Maintenance of the observed moderate (~10%) porosity as CO/CO<sub>2</sub> gas would require an end-stage  $P$  of ~500 bar, far too high for oxidation of C at the low  $f_{\text{O}_2}$  implied by the high- $mg$  silicates.

**References:** [1] McCoy T. et al. 2005. *Ant. Met. Newsl.* 28(2).  
[2] Warren P. H. & Huber H. 2006. Abstract #2400. 37th LPSC.

**GASP! GAS-ASSOCIATED SPHEROIDAL  
PRECIPITATES RELATED TO HASP, FOUND IN  
ANORTHOSITIC APOLLO 14 REGOLITH BRECCIA  
14076.**

Paul H. Warren, Eric Tonui and Edward D. Young. Institute of Geophysics, UCLA, Los Angeles, CA 90095, USA.

The 14076 regolith breccia constitutes roughly half of a 2.0 g pebble. It is far more aluminous (30 wt%  $\text{Al}_2\text{O}_3$ ) than any other Apollo 14 rock [1]. 14076 is extraordinarily rich in spheroidal HASP (high-Al, Si-poor) glasses (and devitrification products) that formed as residues from fractional evaporation of superheated highland impact-melt splashes [1,2]. An issue not yet addressed regarding HASP, is the ultimate fate of the  $\text{SiO}_2$ , FeO and MgO, after evaporation removed them from the flying superheated melt droplets. During a compositional survey of ~60 regolith glass spheroids in 13 mm<sup>2</sup> thin section 14076,5, it became evident that a significant component of the spheroid population is distinctively tiny, and also distinctive in composition. The 30 spheroids smaller than 5  $\mu\text{m}$  are preponderantly the opposite of HASP: nearly pure  $\text{SiO}_2$  (the only two exceptions have apparent  $D = 4\text{-}4.5 \mu\text{m}$ ). The vast majority of these Si-rich spheroids are ~2  $\mu\text{m}$  across — not quite large enough to quantitatively analyze. Only the two largest, 4-5  $\mu\text{m}$  across (the next largest has  $D = 3 \mu\text{m}$ ), yielded good analyses, indicating 96-99 wt%  $\text{SiO}_2$ . However, the problem with the analyses of the smaller spherules is often not so much beam overlap onto outside solids, but overlap onto adjacent regolith porosity, such that the analyses suffer more from low sums than from inaccurate element:element ratios, and the high-Si nature of the true composition is nonetheless manifest. In the intermediate size range (18 spheroids with apparent  $D$  between 5 and 15  $\mu\text{m}$ ), HASP compositions are especially common; e.g., 10 of the 18 have <35 wt%  $\text{SiO}_2$ , and of these, 7 have <24 wt%  $\text{SiO}_2$ . The 13 spheroids larger than ~15  $\mu\text{m}$  (apparent  $D$ ) are preponderantly either “normal” in  $\text{SiO}_2$  or mildly HASP.

As a name for this new type of lunar regolith spheroid, we have chosen GASP, for Gas-Associated Spheroidal Precipitates. It seems highly probable that these materials represent condensates of the mainly  $\text{SiO}_2$ -gas component that was fractionally evaporated out of the associated HASP spheroids.

Besides HASP and the distinctively Si-rich variety of GASP, 14076,5 also contains at least 3 spheroids ( $D = 7\text{-}12 \mu\text{m}$ ) of distinctively FeO-rich composition, 30-38 wt% FeO. The high FeO is accompanied by high  $\text{SiO}_2$  (56-63 wt%) and not by high  $\text{TiO}_2$  (undetectable to 0.04 wt%), so it is hardly likely to represent melt splashes of a mare surface material. The FeO-rich spheroids display quench textures, with constituent minerals far too small for quantitative analysis, but probably dominated by an Fe-rich low-Ca pyroxene (or pyroxenoid) and Si-rich glass. Probably these spheroids also represent condensates of the  $\text{SiO}_2$ - and FeO-rich gas component that was fractionally evaporated out of the associated HASP spheroids. No MgO-rich GASP spheroids were found. Possibly Mg (as the MgO would have evaporated), with an atomic weight of just 24, was less efficiently recondensed than Si and Fe, and instead mainly lost by hydrodynamic escape.

The presence of three different forms of HASP-GASP spheroidal materials all in a single regolith sample (and not, so far, found together anywhere else) suggests that the impact that produced these distinctive materials was relatively small (i.e., not basin-scale).

**References:** [1] Jerde E. et al. 1990. *EPSL* 98, 90-108. [2] Vaniman D. T. & Bish D. L. 1990. *Amer. Min.* 75, 676-686.

### EVIDENCE OF DIFFERING LIQUID REGIMES IN METALLIC MAGMAS.

John T. Wasson. Institute of Geophysics and Planetary Physics, University of California, Los Angeles, CA 90095-1567, USA. E-mail: jtwasson@ucla.edu.

**Introduction:** The magmatic iron meteorites formed by fractional crystallization in kilometer-size bodies of magma. On plots of Ir vs. Au the left envelope of the scatter field defines the location of the solid crystallization track. The liquid crystallization track can be inferred because some members of each group formed as mixes of equilibrium solids and trapped melt [1]. The equation currently used to model the crystallization is simplified version of eq. (8) of Chabot and Jones [2]

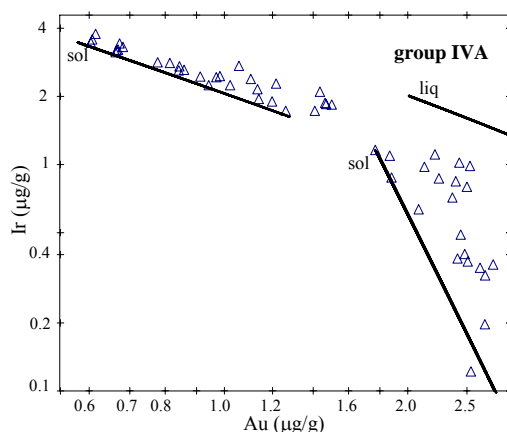
$$\log D = \log D_0 - \beta \log [(1 - 2X_S - 3X_P)/(1 - X_S - X_P)] \quad (1).$$

The key terms are  $D$ , the solid/liquid distribution ratio and  $\beta$ , the slope showing the change in  $D$  with changing nonmetal content of the magma;  $X_S$  and  $X_P$  are mole fractions.

Wasson et al. [3] recently noted that, in order to obtain good fits to the data sets they needed very different values of the intercepts  $D_0$ . For groups such as IID and IVA with low nonmetal contents they require  $D_0$  values for Ir are around 1.7; for groups with moderately high nonmetal contents (IIAB and IIIAB) the  $D_0$  values for Ir are near 4.5.

Here we call attention to the rapid change in slope within group IVA; at a Au content of about 1.6  $\mu\text{g/g}$  corresponding to ~60% crystallization of the magma the slope changes within a small range in Au contents. At this point the S and P contents of the magma had increased by factors of ~2.5.

We suggest that this large change reflects the transition between two melt regimes; at low S and P concentrations the nonmetals seem to have relatively minor effects on  $D$  values, but at the higher values (above Au = 1.6  $\mu\text{g/g}$ ) the liquid enters a different chemical-physical regime in which the change in  $D$  value is much more pronounced. In the Figure we show two solid tracks and one liquid track; the second liquid track is offscale.



**References:** [1] Wasson J. T. 1999 *Geochim. Cosmochim. Acta* 59, 115; [2] Chabot N. L. and Jones J. H. 2003 *Meteorit. Planet. Sci.* 38, 1425; [3] Wasson J. T., Huber H. and Malvin D. J. 2006 *Geochim. Cosmochim. Acta* 70, submitted.

### NEBULAR FINES, PRESOLAR GRAINS AND COLLATERAL DAMAGE DURING CHONDRULE FORMATION.

John T. Wasson. Institute of Geophysics and Planetary Physics, University of California, Los Angeles, CA 90095-1567, USA. E-mail: jtwasson@ucla.edu.

**Introduction:** Paul Pellas once said that St. Mesmin was not a meteorite but a meteorite collection. Many of the chondrules in LL3.0 Semarkona and other primitive chondrites are not just chondrules, they contain so many relict grains that they could be called chondrule collections. Each relict grain is a fragment of an earlier chondrule, and frequently different chondrule precursors are represented. This and other evidence shows that (at least in the ordinary chondrite formation region) chondrule matter experienced several flash-heating events that raised temperatures high enough to melt chondritic silicates. The mechanism that formed chondrules is still not known, but there is little doubt that it heated both the chondrule precursors and the associated gas and dust to create a plasma with a temperature in excess of 2000 K, high enough to permit rapid heat conduction into 10- $\mu$ m grains. It is important to determine if nebular fines (“matrix”) experienced the same number of high-temperature events, and how this relates to the composition of the fines and the observed abundance of presolar grains.

**Vaporization versus survival of presolar grains.** Wasson [1] noted that the temperature at which olivine vaporizes is  $\sim 1300$  K,  $>600$  K lower than that achieved in the chondrule-melting plasmas. Because evaporation occurs one layer at a time, tiny matrix grains will evaporate even though the chondrules lose relatively trivial mass fractions.

A reasonable working assumption is that 90% of nebular fines have passed through a hot plasma; in these parcels micrometer-size olivine and more volatile silicates evaporated. A key question is then what happened to presolar grains. The abundance of presolar diamonds and SiC in Semarkona and other low-type-3 ordinary chondrites is  $\sim 100$   $\mu$ g/g [2]. Is it reasonable that this is a remnant population, and that  $\sim 90\%$  of the original inventory has been destroyed? The two possible answers are 1) yes, and 2) no, these refractory grains are more resistant to evaporation.

**Late versus early presolar matter.** The nebula was continuing to accrete during the period of chondrule formation; accretion powered the turbulence that hindered the formation of planetesimals and led to grain-gas segregations of the sort recorded in the metal-silicate fractionation within the ordinary-chondrite suite. It seems likely that nebular fines within primitive chondrites are themselves a mixture of a) late arriving presolar matter, most of which has not been immersed in a chondrule-forming plasma; and b) a much larger fraction which largely consisted of smoke-like particles that formed by flash evaporation and rapid condensation during chondrule formation.

Alexander [3] inferred that chondritic fines consist of slightly modified interstellar matter that is very closely related to the matter in CI chondrites. My view is very different. I suspect that CI chondrites are not grail-like, but samples of largely recycled fines from one particular nebular time and place.

**References:** [1] Wasson J. T. 1996 *Chondrules Protoplanetary Disk*, 45; [2] Huss G. R. and Lewis R. S. 1995 *Geochim. Cosmochim. Acta* 59, 115; [3] Alexander C. 2005. *Meteorit. Planet. Sci.* 40, 973

**SULFIDE-METAL NODULES IN EH3 CHONDRITES.**

M. K. Weisberg<sup>1,2</sup>, H. C. Connolly<sup>1,2</sup>, D. S. Ebel<sup>2</sup> and M. Kimura<sup>3</sup> <sup>1</sup>Dept. Physical Sciences, Kingsborough College CUNY, Brooklyn, NY 11235. mweisberg@kbcc.cuny.edu. <sup>2</sup>Dept. Earth and Planetary Sciences, American Museum Natural History, NY, NY 10024. <sup>3</sup>Ibaraki University, Mito 310-8512, Japan.

**Introduction:** The enstatite chondrites (EC) have highly reduced mineral assemblages [e.g., 1] that likely formed in equilibrium with a reducing vapor. Another intriguing aspect of the EC is that they appear to share the same oxygen isotopic reservoir as the Earth and Moon [2, 3]. A wide variety of sulfide-metal assemblages in EC record primary and secondary processes [4]. Here we focus on the origin of sulfide-metal nodules in Sahara 97096 and Kota Kota (both EH3) in relation to chondrule formation and nebular condensation under reduced conditions. We previously described sulfide-metal nodules in Sahara 97096 [5].

**Results:** Sahara 97096 and Kota Kota are among the most primitive EH3 chondrites, based on modal abundances (>6 vol.%) and compositions (>0.2 wt.% Cr<sub>2</sub>O<sub>3</sub>) of their olivine [6]. Sulfide-metal nodules are roughly circular in thin section with sharp, well-defined boundaries. Nodule sizes range from ~50 to 300 μm, slightly smaller than the chondrules (up to ~700 μm). Sulfide-metal nodules contain a wide variety of sulfides including troilite ± oldhamite (CaS), ± niningerite [(Mg,Fe,Mn)S], ± ferroan sphalerite [(Zn,Fe)S], ± djerfisherite [(K,Na)<sub>6</sub>(Cu,Fe,Ni)<sub>25</sub>S<sub>26</sub>Cl], in association with Si-bearing kamacite ± schreibersite, ± perryite [(Ni,Fe)<sub>x</sub>(Si,P)<sub>y</sub>]. Many of these sulfides are also present in EH3 chondrules. Troilite is generally the most common sulfide in the nodules ± exsolution of daubreelite [(Fe,Cr)<sub>2</sub>S<sub>4</sub>]. Schreibersite generally occurs as small inclusions in oldhamite or niningerite and occasionally in troilite. Nodules generally contain ubiquitous grains of silica and enstatite. Some have small amounts of graphite. One unusual nodule in Kota Kota contains 7 vol.% ferroan sphalerite and small grains of a Na-rich feldspathic component. Some nodules have concentric layered structures with oldhamite or niningerite cores, as previously reported [7].

**Discussion and Conclusions:** Sulfide-metal nodules are sensitive indicators of metamorphism of E3 chondrites. Oldhamite is predicted to be the highest-temperature Ca-bearing phases to condense from a cooling solar gas under reducing conditions [8], consistent with its occurrence in the cores of some layered nodules [7] and its enriched REE abundances [9]. Sulfide-metal nodules may be the equivalent of refractory inclusions under reducing conditions. Alternatively, the nodules formed as immiscible sulfide-metal liquids during chondrule formation.

**References:** [1] Keil K. 1968. *Journal of Geophysical Research* 73:6945-6976. [2] Clayton R. N. and Mayeda T. K. 1984. *Journal of Geophysical Research* 89:C245-C249. [3] Javoy M. 1995. *Geophysical Research Letters* 22:2219-2222. [4] El Goresy A. et al. 1988. *Proceedings NIPR Symposium Antarctic Meteorites* 1:65-101. [5] Weisberg M. K. and Prinz M. 1998. Abstract # 1741. 29th *Lunar & Planetary Science Conference*. [6] Weisberg M. K. et al. 2005. Abstract # 1420. 36th *Lunar & Planetary Science Conference*. [7] Lin Y. and El Goresy A. 2002. *Meteoritics and Planetary Science* 37: 577-599. [8] Larimer J. W. and Bartholomay M. 1979. *Geochimica et Cosmochimica Acta* 43:111-120. [9] Crozaz G. and Lundberg L. L. 1995. *Geochimica et Cosmochimica Acta* 59:3817-3831.

**COSMOGENIC RADIONUCLIDES IN A WEATHERED, 2.8 MILLION YEAR OLD H-CHONDRITE FOUND ON TOP OF FRONTIER MOUNTAIN, ANTARCTICA.**

K. C. Welten<sup>1</sup>, K. Nishiizumi<sup>1</sup>, L. Folco<sup>2</sup>, and M. W. Caffee<sup>3</sup>.  
<sup>1</sup>Space Sciences Laboratory, University of California, Berkeley, CA 94720, USA. E-mail: kcwelten@berkeley.edu. <sup>2</sup>Museo Nazionale dell'Antartide, 53100 Siena, Italy; <sup>3</sup>PRIME Lab, Purdue University, West Lafayette, IN 47907, USA.

**Introduction:** In 2001, a small (1.5 g) chondrite was found on top of Frontier Mountain (FRO) during a geomorphological survey by a PNRA team. The meteorite was found on a glacially eroded bedrock surface at an altitude of 2775 m (i.e., ~600 m above present day ice level). The meteorite, FRO 01149, is an H4 chondrite [1], and shows almost complete oxidation of the metal and sulfides. Preliminary cosmogenic <sup>10</sup>Be and <sup>41</sup>Ca results indicated a terrestrial age >0.5 Myr and possibly >2 Myr [2]. However, the lack of metal and possible contamination of the meteorite with terrestrial ("meteoric") <sup>10</sup>Be and <sup>36</sup>Cl made the interpretation of these results difficult. We therefore carried out leaching experiments to remove the weathering products, and measured <sup>10</sup>Be, <sup>26</sup>Al and <sup>36</sup>Cl in the leached silicate grains.

**Experimental:** After crushing the meteorite to <0.5 mm, we leached ~150 mg in 6N HCl. After leaching for 10 min. at ~25 °C, we dissolved 31 mg of the residue (R1) for radionuclide analysis. The remaining fraction was then leached for 30 min. in 6N HCl at ~50 °C. The residue was rinsed and two aliquots, of 27 mg (R2, <125 μ) and 4 mg (R3, <125 μ), and a duplicate sample of 18 mg (R4) were dissolved for radionuclide analysis by AMS.

**Results and discussion:** Chemical analysis of the four samples shows that leaching at ~25 °C removed only half of the oxidized FeNi-metal (R1), whereas leaching at ~50 °C (R2-R4) removed >99% of the weathering products. The latter was confirmed by microprobe analyses and BSE imaging of the leached grains. The <sup>10</sup>Be and <sup>26</sup>Al concentrations in R2-4 show average values of 6.2±0.2 and 3.8±0.2 dpm/kg, respectively. These concentrations and the average <sup>26</sup>Al/<sup>10</sup>Be ratio of 0.61±0.02 correspond to a terrestrial age of 2.82±0.10 Myr. The average <sup>36</sup>Cl concentration of 0.057±0.013 dpm/kg in two leached samples (R2,R4) only yields a minimum age of ~2 Myr, since part of the <sup>36</sup>Cl is due to *in-situ* production on Earth, which is estimated at ~0.03 dpm/kg (15 atoms/g/year) at an altitude of 2775 m [3].

The <sup>26</sup>Al/<sup>10</sup>Be ratio of ~0.41 in the bulk sample is ~30% lower than in the leached samples. This low value is due to contamination with ~2.4 dpm/kg of meteoric <sup>10</sup>Be, which was incorporated in the meteorite upon oxidation of the metal. Similarly, the high <sup>36</sup>Cl concentrations of ~0.8 dpm/kg in the bulk sample and ~0.5 dpm/kg in R1 are also due to "meteoric" <sup>36</sup>Cl. The terrestrial <sup>10</sup>Be and <sup>36</sup>Cl components correspond to a <sup>10</sup>Be/<sup>36</sup>Cl ratio of ~7.4, within the range of 5-20 found in polar ice samples.

**Conclusion.** With a terrestrial age of ~2.8 Myr, FRO 01149 is the oldest stony meteorite found on Antarctica [4,5]. Its location of find and high degree of weathering suggests it is a local fall and constrains the last overriding of Frontier Mountain. Preliminary results of *in-situ* <sup>10</sup>Be in quartz from the granitic bedrock surface show a minimum exposure age of ~1.2 Myr.

**References:** [1] Russell S. et al. 2002. *Meteoritics & Planetary Science* 37, A157-A182. [2] Folco L. et al. 2004. *Meteoritics & Planetary Science* 39, A40. [3] Gosse J. & Phillips F. 2001. *Quaternary Science Review* 20, 1475-1560. [4] Scherer P. et al. 1997. *Meteoritics & Planetary Science* 32, 769-773. [5] Welten K. et al. 1997. *Meteoritics & Planetary Science* 32, 775-780.

### THE COMPLEX EXPOSURE HISTORY OF A LARGE L6 CHONDRITE SHOWER FROM OMAN.

K. C. Welten<sup>1</sup>, K. Nishiizumi<sup>1</sup>, D. J. Hillegonds<sup>2</sup> and M. W. Caffee<sup>3</sup>. <sup>1</sup>Space Sciences Laboratory, University of California, Berkeley, CA 94720, USA (e-mail: kcwelten@berkeley.edu), <sup>2</sup>CAMS, Lawrence Livermore National Laboratory, Livermore, CA 94550, USA, <sup>3</sup>PRIME Lab, Purdue University, West Lafayette, IN 47907, USA.

**Introduction:** Most of the large chondrites, like Bur Gheluai, Gold Basin, Jilin, QUE 90201 and Tsarev reveal complex exposure histories with a first stage on the parent body and a second stage of 0.4 to 20 Myr in space. Recently, a large L6 chondrite strewnfield, JaH 073, was found in Oman [1]. This well documented shower contains ~3000 fragments with a total mass of ~550 kg. Preliminary noble gas results show low <sup>22</sup>Ne/<sup>21</sup>Ne ratios and a factor of 15 variation in the <sup>21</sup>Ne concentration, indicating a large pre-atmospheric size and possibly a complex exposure history [2]. To investigate its cosmic-ray exposure history in more detail we measured cosmogenic <sup>10</sup>Be, <sup>26</sup>Al and <sup>41</sup>Ca in ten fragments of this shower.

**Experimental Methods:** We crushed the meteorite samples and leached silicate grains >0.25 mm for 30 min. in 6N HCl to remove weathering products. The leached samples were then rinsed and dissolved in HF/HNO<sub>3</sub> for radionuclide analysis. Concentrations of <sup>10</sup>Be and <sup>26</sup>Al were measured at Purdue, those of <sup>41</sup>Ca were measured at LLNL.

**Results and discussion:** Concentrations of <sup>41</sup>Ca range from 6 to 35 dpm/kg. The high <sup>41</sup>Ca contents in the JaH 073 samples are due to neutron-capture <sup>41</sup>Ca contributions, which range from ~0.2 to 1.8 dpm/gCa. The maximum value of 1.8 dpm/gCa can only be acquired in objects with radii of 50-200 cm, thus confirming the large pre-atmospheric size of JaH 073 [1,2].

The <sup>10</sup>Be and <sup>26</sup>Al concentrations range from 7.6-12.8 dpm/kg and 45-64 dpm/kg, respectively, while the <sup>26</sup>Al/<sup>10</sup>Be ratio ranges from 4 to 6. Interestingly, the <sup>26</sup>Al/<sup>10</sup>Be ratio is inversely correlated with the <sup>10</sup>Be concentration (Fig. 1). This trend is similar to the one observed in Jilin and suggests a complex exposure history with a long exposure on the parent body, followed by a relatively short exposure (~1.0 Myr) as a large object in space. This scenario corroborates the trend that many large chondrites were exposed on their parent body before ejection into space.

**References:** [1] Gnos E. et al. 2003. *Meteoritics & Planetary Science* 38, A31. [2] Huber L. et al. 2006. *Lunar and Planetary Science Conference* 37. CD-ROM, #1628.

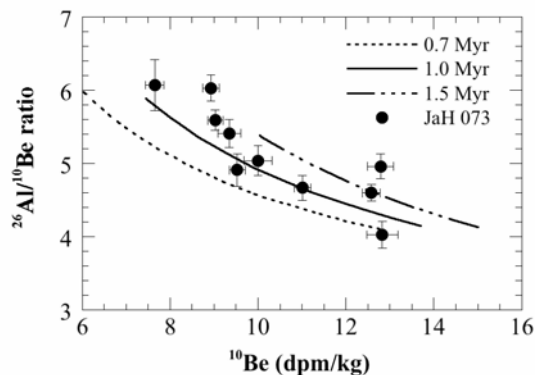


Fig. 1. Measured <sup>26</sup>Al/<sup>10</sup>Be vs. <sup>10</sup>Be in JaH 073, compared to calculated values for 2<sup>nd</sup>-stage exposure times of 0.7-1.5 Myr.

### IMPACT-RELATED DEFORMATION IN THE COLLAR ROCKS OF THE VREDEFORT DOME, SOUTH AFRICA.

Frank Wieland\*, Roger L. Gibson, and Wolf Uwe Reimold, Impact Cratering Research Group, School of Geosciences, University of the Witwatersrand, Private Bag 3, P.O. Wits 2050, Johannesburg, South Africa \*Corresponding author (fwieland@ix.urz.uni-heidelberg.de)

**Introduction:** The Vredefort Dome represents the deeply eroded remnant of the eroded central uplift of the world's oldest (2.02 Ga ) and largest (ca. 300 km) known impact structure [1]. It comprises an ~40 km wide core of Archean basement gneisses and an ~20 km wide collar of subvertical to overturned Late Archaean to Paleoproterozoic supracrustal strata. We report on the results of a detailed structural geological study of the supracrustal strata of the inner collar of the Dome.

**Results:** Contrary to the findings about shatter cones of some earlier workers in the Vredefort structure [2, 3], the Vredefort cone fractures do not show uniform apex orientations at any given outcrop. The model of simple back-rotation of the strata to a horizontal pre-impact position does not lead to a uniform centripetal-upward orientation of the cone apices. Striation patterns on the cone surfaces are variable, ranging from typically diverging, i.e., branching off the cone apex, to subparallel to parallel on almost flat surfaces and striation angles do not increase with distance from the crater center, as suggested previously [4]. Pseudotachylitic breccias in the collar rocks occur as up to several centimeter-wide veins with variable orientations to the bedding and as more voluminous pods and networks in zones of structural complexity, such as the hinges of large-scale folds and along large-scale faults. This study revealed a highly heterogeneous internal structure of the collar involving folds, faults, fractures and melt breccia occurrences that are interpreted as the product of shock deformation and central uplift formation during the Vredefort impact event. Broadly radially-oriented symmetric and asymmetric folds, with wavelengths from tens of meters to kilometers, and conjugate radial to oblique faults with strike-slip displacements of, typically, tens to hundreds of meters accommodated tangential shortening of the collar of the dome that decreased from ~17 % at a radial distance from the dome center of 21 km, to <5 % at a radial distance of 29 km.

In addition to shatter cones, quartzite units show two other fracture types – a centimeter-spaced rhomboidal to orthogonal type that may be the product of shock-induced deformation and related to the formation of shatter cones, and later joints accomplishing tangential and radial extension.

**Conclusions:** Based on these results, it is possible to establish a temporal sequence of deformation events. Shatter cones and related closely-spaced fractures were formed during the shock phase of the cratering process. The formation of, at least some, shock-induced pseudotachylitic breccia also belongs into this phase. Large-scale folds and faults, and friction-generated melts can be related to the initial formation of the central uplift, and formation of extensional joints to the subsequent collapse of the central uplift.

**References:** [1] Gibson, R.L. and Reimold, W.U. (2001): *Memoir '92*, Council for Geoscience, 111pp.; [2] Manton (1962a): MSc Thesis (unpubl.), Univ. Witwatersrand, Johannesburg, 167pp.; [3] French 1998: *Lunar and Planet. Inst. Houston, Contrib. No. 954*, 120pp.; [4] Sagy et al. (2004): *J. Geophys. Res.* 109:B10209.

### WHAT ARE THE CONSEQUENCES IF THE "SEP" SOLAR NOBLE GAS COMPONENT DOES NOT EXIST?

R. Wieler<sup>1</sup>, A. Grimberg<sup>1</sup>, and V. S. Heber<sup>1</sup>. <sup>1</sup>ETH Zürich, Isotope Geology, NW C84, CH-8092 Zürich, Switzerland. wieler@erdw.ethz.ch

Lunar dust grains appear to contain a solar noble gas component isotopically heavier than the solar wind (SW) and implanted to larger depths. This component was attributed to solar particles implanted at considerably higher energies than the SW [1, 2], and dubbed "SEP" for Solar Energetic Particles [2]. Supportive evidence came from analyses of solar energetic particles from coronal mass ejections, which also suggested <sup>20</sup>Ne/<sup>22</sup>Ne on average possibly to be lower than the SW value [3]. However, it has been difficult to reconcile the high apparent abundance of SEP in lunar samples with the very low measured flux of solar energetic particles, hence the suspicion that "SEP" may be an artifact caused by isotope-dependent penetration depths or diffusion [e. g. 4, 5].

Data from a metallic glass exposed on the Genesis mission now seem to have clarified this conundrum [6]. The depth profile of <sup>20</sup>Ne/<sup>22</sup>Ne in the glass is very similar to that predicted for an isotopically uniform SW component implanted with the velocity distribution measured by Genesis. Thus, the gases at larger depths in all probability do not represent an isotopically distinct component.

Here we discuss some implications of this finding in geo- and cosmochemistry. In many cases, consequences are not dramatic. Often, measured isotopic compositions of solar gases heavier than the pure SW, rather than implying a prominent contribution of SEP, now indicate a relative enrichment of (isotopically heavy) fractionated SW from larger depths, due to e.g. loss of outermost grain layers. Further work will have to clarify whether young lunar grains in sputter-saturation equilibrium conserve the true SW isotopic composition at the very surface, as postulated [7], but first Genesis data [8] appear to confirm previous SW compositions based on lunar samples. The isotopic composition of Ne in the Earth's mantle has been interpreted to reflect grains containing a mixture of SW-Ne and SEP-Ne added to the accreting Earth [9]. Now, as in the lunar regolith, this putative "Ne-B" would be reinterpreted as enrichment of fractionated SW-Ne due to partial grain surface erosion. A similar enrichment now seen in deeper layers in lunar grains [7] will not necessarily affect the alternative interpretation of these data by [10], who suggest that some volatiles in the lunar regolith originate from the Earth's atmosphere. Oxygen lighter than the terrestrial atmosphere in lunar metal grains has been interpreted as representing SEP-oxygen [11]. Being viewed now as high-speed SW-oxygen instead, the inference by [11] about the isotopic composition of solar-nebula O would not need to be revisited, because the depth-dependent fractionation of SW species remains identical to the previously supposed fractionation between SW and SEP.

**References:** [1] Black D. C. and Pepin R. O. 1969. *Earth Planet. Sci. Lett.* 6:395-405 [2] Wieler R. et al. 1986. *Geochim. Cosmochim. Acta* 50:1997-2017. [3] Leske R. A. et al. 1999. *Geophys. Res. Lett.* 26, 2693-2696. [4] Frick U. et al. 1988. *Proc. Lun. Planet. Sci. Conf.* 18<sup>th</sup>, 87-120. [5] Mewaldt R. A. et al. 2001. *AIP Conf. Proc.* 598:393-398. [6] Grimberg A. et al. 2006. *Lunar Planet. Sci.* XXXVII, #1782. [7] Heber V. S. et al., *Astrophys. J.* 597:602-614. [8] Meshik A. P. et al. 2006. *Lunar Planet. Sci.* XXXVII, #2433. [9] Trierloff M. et al. 2000. *Science* 288:1036-1038. [10] Ozima M. et al. 2005. *Nature* 436:655-659. [11] Hashizume K. and Chaussidon M. 2005. *Nature* 434:619-622.

**THE EFFECT OF ATMOSPHERIC ENTRY HEATING ON MICROMETEORITE VOLATILE COMPOSITION.**

R. C. Wilson, V. K. Pearson, I. A. Franchi, I. P. Wright and I. Gilmour. Planetary and Space Sciences Research Institute, Open University, Milton Keynes, UK. E-mail: r.c.wilson@open.ac.uk.

**Introduction:** With estimates of present day mass flux of  $40,000 \pm 20,000$  t/yr [1], micrometeorites (MMs) may have served as a substantial contributor of volatiles and biologically significant molecules to the early Earth (or other young planetary surfaces). These particles have high relative velocities, which dissipate their energy during atmospheric entry. This study investigates the effect of heating during atmospheric entry, on the survival and modification of organic material in MMs, and their involvement in pre-biotic organic chemistry.

**Experimental Techniques:** Due to the micrometer-sized nature of MMs and their low availability for analysis, compositionally analogous materials are required to represent unmelted MM particles. In this case, 9mg aliquots of the powdered carbonaceous chondrite Murchison are used.

The samples were heated in air to peak temperatures between 400 and 1000°C for the short durations of 5, 10 and 20 seconds, using a platinum filament fitted to a CDS 1000 pyroprobe. A thermocouple was embedded in the sample to quantify the peak temperature experienced by the sample. The heating range is comparable to the peak temperatures experienced by unmelted MMs [2, 3]. Fractions of the heated sample were examined using elemental and thermo-gravimetric (TG) analysers, to assess the percentage carbon loss and volatile and organic survival.

**Results:** Elemental analysis demonstrates that the shorter the heating duration, the higher the percentage of total carbon surviving any peak entry heating temperature. A minimum of 5% total carbon remains in samples heated to ~900°C for 20s, corresponding to carbonate minerals. A minimum of 30% total carbon remains in samples heated to a similar peak temperature for 5s. The remaining carbon is dominated by carbonate minerals with detectable quantities of organics.

A greater abundance and broader range of organic material survives in samples exposed to higher entry heating temperatures at shorter heating durations. As TG CO<sub>2</sub> profile peaks corresponding to organics are very broad, it is not possible to identify individual organic components. Alternative techniques are required to determine the nature of surviving organic material.

Similarly, at shorter heating durations, a greater abundance of adsorbed and structurally bound water was able to survive, when exposed to higher entry heating temperatures. The structural water peaks are consistent with cronstedtite [4], a dominant phyllosilicate present in Murchison [5].

**Implications:** The results demonstrate that organic molecules and other volatile components can withstand certain atmospheric entry heating conditions. It is therefore plausible that micrometeorites may have made a contribution to the organic inventory of the early Earth, prior to the evolution of life.

**References:** [1] Love, S. G. and Brownlee, D. E. 1993. *Science* 262:550-553. [2] Toppani, A. et al. 2001. *Meteoritics and Planetary Science* 36:1377-1396. [3] Love, S. G. and Brownlee, D. E. 1991. *Icarus* 89:26-43. [4] Morris, A. A. et al. 2005. Abstract #1925. 36th Annual Lunar and Planetary Science Conference [5] Buseck, P. R. and Hua, X. 1993. *Annual Review of Earth and Planetary Sciences* 21:255-305.

## IMPLICATIONS FOR THE CHICXULUB FIREBALL DERIVED FROM A SYSTEMATIC ANALYSIS OF ITS DEPOSITS.

A. Wittmann<sup>1</sup>, D. Stöffler<sup>1</sup>, L. Hecht<sup>1</sup>, T. Kenkmann<sup>1</sup>. <sup>1</sup>Museum für Naturkunde, Mineralogie, Invalidenstr. 43, 10115 Berlin, Germany. axel.wittmann@museum.hu-berlin.de

**Introduction:** A continuous record of the Chicxulub fireball deposits is intersected in the ICDP-Chicxulub Yaxcopoil-1 (Yax-1) drilling that is located in the structure's annular moat, ~60 km SSE' from the crater's center [1]. Systematic, image analysis-based study of this 100 m sequence of suevite-like rocks was conducted on photographs of half-cores and thin sections of ~40 samples to reconstruct emplacement conditions of these impact breccias.

**Samples and Methods:** Modal abundance of components and particle shape parameters were determined for the lapilli particle size range recorded in the half-cores. Bulk chemical compositions were derived from EMP analyses of 90 impact melt particles (MP).

**Results:** Five MP types were distinguished. The first type was rapidly quenched and is only abundant in the uppermost units and in dike breccias. The second type is variably quenched, rich in vesicles, and exhibits shard morphologies, thus indicating airborne transport. This MP type only occurs in the upper four units that are interpreted as airfall suevites. The third MP type is thoroughly crystallized with Pl and Cpx phenocrysts and is the most abundant MP type in the three basal units that overlie sedimentary megablocks. In these units, shape parameters of these MP indicate thermal softening and some corroded rims, suggesting post-depositional temperatures >~700°C [2]. The fourth MP type bears abundant Fe-O crystals and is only abundant in the airfall suevites. This suggests fO<sub>2</sub> conditions in excess of the FMQ-buffer for the formation of this MP type [3]. The variation in bulk chemical compositions of the MP is more pronounced on the unit-level than between particle types. This could suggest a homogenized impact melt that underwent compositional differentiation due to alteration and variable degrees of quenching. Carbonate target clasts in the lower airfall suevites and the impact melt unit indicate contact metamorphism. Below the impact melt unit, carbonate occurs with melt textures [1]. Particle size distributions in the uppermost unit agree with models for condensation from an impact vapor plume [4]. Distinct sorting is only indicated in the uppermost unit. Alignments of MP indicate increasing turbulence with depth and melt injections in dikes.

**Conclusions:** Petrologic characteristics of MP in Yax-1 suggest variable fO<sub>2</sub> and T-t conditions during their formation: Shape parameters indicate sorting processes, alignments and modifications of MP. Indications for thermal alteration of the MP above ~700°C and reworking features suggest the presence of a hot region of the fireball that collapsed with an erosive surge after the deposition of a melt unit that capped a ground-surgéd ejecta curtain deposit. Melt textures indicate that degassing of anhydrite and carbonate was inhibited below the melt unit.

**References:** [1] Stöffler, D. et al. 2004. *Meteoritics & Planetary Science* 39:1035-1067. [2] von Engelhardt et al. 1995. *Meteoritics & Planetary Science* 30:279-293. [3] Frost, B. R. 1991. *Reviews in Mineralogy* 25:1-9. [4] de Niem, D. 2002. *GSA Special Paper* 356:631-644.

**STEPWISE CHEMICAL DISSOLUTION OF CARBONACEOUS CHONDRITES: CORRELATIONS BETWEEN VOLATILE TRACE ELEMENTS AND MAJOR/MINOR MINERAL CONSTITUENT ELEMENTS.**

S. F. Wolf. Dept. of Chemistry, Indiana State University, Terre Haute, IN 47809-5901. E-mail: wolf@indstate.edu.

**Introduction:** In an effort to gain a greater understanding of the distribution and cosmochemical affinity of volatile trace elements (VTEs) within primitive meteorites we are performing stepwise chemical dissolution of homogenized bulk samples of the carbonaceous chondrites Allende (CV3) and Murchison (CM2). Previously we reported preliminary results from these experiments examining fractional releases of the highly VTEs Cd, Bi, Tl and In [1]. Here we examine releases for the complete dissolution experiment for these highly VTEs, several additional VTEs (Cu, Ag, Ga, Rb, Cs, Se, Te, Zn and Pb) and correlations between releases of these elements and the releases of major/minor mineral constituent elements (Na, Mg, Al, Si, P, S, K, Ca, Ti, Cr, Mn, Fe, Co and Ni). We use multivariate factor analysis and cluster analysis to determine whether or not there are correlations in the release patterns of the VTEs and the major/minor mineral constituent elements. Afterward, we interpret these correlations as indirect evidence of the identity of the VTE-containing host phase or phases.

**Methods:** We use a modified dissolution procedure based on the method of Podosek et al. [2] in which 1-g aliquots of powdered homogenized samples of each meteorite were treated with increasingly aggressive reagents: H<sub>2</sub>O, 9 M CH<sub>3</sub>COOH, 4 M HNO<sub>3</sub>, 6 M HCl, HF/HCl, HNO<sub>3</sub>/HCl, and HClO<sub>4</sub>. Leachates were analyzed by ICPMS and fractional releases relative to bulk concentrations were calculated as described in [1].

**Results:** Measured releases of major/minor elements are consistent with non-stoichiometric dissolution of a complex mixture of mineral phases. Releases of VTEs indicate that as a group they are dispersed heterogeneously with respect to their host phases. Releases of the highly VTEs Pb, Cd, Bi, Tl and In are consistent with the presence of multiple volatile-rich, chemically fractionated, low-temperature phases. Factor analysis of elemental releases show that five factors account for 91% of the variance of the elemental release data. Analysis of factor loadings reveal clusters of elements possessing correlated fractional releases, resulting presumably from dissolution of the same mineral phase or suite of mineral phases. The largest cluster loaded on factor F1 comprising major/minor elements Na, Mg, Al, K, Ca, Mn and Fe. This cluster apparently represents lithophile behavior. Included in this group of lithophiles are the highly VTEs Cd and In. The second significant cluster loaded primarily on Factor F2 and comprised siderophiles Ni and Co along with the VTEs Cu, Te, Pb, Bi and Tl. Chalcophile elements including S and Se clustered on Factor F3. Fractional release patterns for S were consistent with multiple S-containing phases including a water-soluble sulfate phase (in Murchison), a HNO<sub>3</sub>-soluble phase and a HNO<sub>3</sub>/HCl-soluble phase (in both Allende and Murchison). Further partial-dissolution experiments are in progress to determine whether the highly VTEs are preferentially sited on the exterior of grain boundaries. Together, our data should help elucidate some of the complex cosmochemical processes that led to the final distribution of VTEs in primitive meteorites.

**References:** [1] Wolf S. F. 2005. *Meteoritics & Planetary Science* 40:A169. [2] Podosek F. A. et al. 1997. *Meteoritics & Planetary Science* 32:617-627.

### ANALYSIS OF RESIDUES RESULTING FROM MAFIC SILICATE IMPACTS INTO ALUMINIUM 1100

P. J. Wozniakiewicz<sup>1, 2</sup>, A. Kearsley<sup>1</sup>, M. J. Burchell<sup>3</sup>, M.J. Cole<sup>3</sup>, P. A. Bland<sup>2</sup>. <sup>1</sup>IARC, Dept. of Mineralogy, The Natural History Museum, London SW7 5BD, UK. E-mail: p.wozniakiewicz@nhm.ac.uk. <sup>2</sup>IARC, Dept. of Earth Sci. and Eng., Imperial College London, South Kensington Campus, London SW11 3RA, UK. <sup>3</sup>School Phys. Sci., University of Kent, Canterbury, Kent CT2 7NR, UK.

**Introduction:** The Al 1100 foils on the Stardust spacecraft had the primary function of securing the aerogels in place, however they also provided an extra surface totaling 153cm<sup>2</sup> [1] upon which cometary materials may be examined, in the form of impact residues. Their collection will provide flux information for particles  $\leq 1\mu\text{m}$  in size that cannot easily be found and extracted from aerogel, as well as compositional information on a wide size range of impacting particles.

Earlier work [2] suggests that residues should be plentiful from impacts at Stardust encounter velocities (~6.1km/s), however, little is known about how the materials will have changed during impact. Fully exploiting this unique opportunity requires that we understand the impact process occurring on the foils; and in particular, whether it is possible to distinguish the most important minerals expected within cometary materials.

**Experimental Methodology:** For this study, a series of light gas gun shots were conducted at the University of Kent, firing magnesium silicate minerals into Stardust foils. An Mg-rich olivine, enstatite, diopside and lizardite were chosen as representative of minerals likely to be contained within comets [3]. Residues from 5 craters for each of these magnesium silicates were then analysed using SEM EDS at the Natural History Museum. As the residue thickness and geometry (a thin sheet on a sloping interior crater wall) differ from the form of conventional microanalysis standards, creating a relatively short matrix absorption pathway, it was not considered appropriate to use the matrix correction routines used for normal quantitative electron microprobe analyses. The raw magnesium and silicon counts were therefore compared against those for their precursor projectiles. The Mg to Si ratio was chosen for comparison as it provides an excellent, but simple means by which to distinguish between these important cometary dust components.

**Results and Discussion:** A small but systematic increase in Mg counts relative to Si is seen for all residues when compared to projectile compositions. However, in our graphical plots, the minerals remain distinct from one another in both projectile and residue composition. We conclude that the main groups of anhydrous mafic silicates should be easily and reliably distinguishable in EDS analyses taken from within Stardust foil craters, suggesting that a valuable additional collection of cometary materials is available to researchers. We are now extending our study to recognition and in situ analyses of other silicate, sulfide, carbonate and oxide minerals of importance in extraterrestrial samples.

**References:** [1] Tsou P., Brownlee D. E., Sandford S. A., Hörz F., Zolensky M. E. 2003. *Journal of Geophysical Research (Planets)* 108(E10): 8113, 10.1029/2003JE002109 [2] Bernhard R. P. and Hörz F. 1995. *International Journal of Impact Engineering* Vol. 17. pp.69-80 [3] Hanner M. S. 2003. In: Henning T. (ed.) *Astromineralogy*. pp. 171-188.

**PLANETESIMAL FORMATION INDUCED BY PHOTOPHORESIS AT THE INNER EDGE OF THE SOLAR NEBULA.**

G. Wurm<sup>1</sup>, O. Krauss<sup>1</sup>, H. Haack<sup>2</sup>. <sup>1</sup>Institut für Planetologie, Wilhelm-Klemm-Str. 10, D-48149 Münster, Germany, E-mail: gwurm@uni-muenster.de. <sup>2</sup>Natural History Museum of Denmark, Øster Voldgade 5-7, DK-1350 Copenhagen K, Denmark.

**Introduction:** Studies of <sup>26</sup>Al in eucrites and mesosiderites show that large planetesimals accreted shortly after the Solar Nebula formed, probably in much less than 1 Myr and before chondrite parent bodies formed [1]. Recent dynamical studies and interpretations of observations of asteroids suggest that differentiated bodies in the main asteroid belt originally formed closer to the sun and were scattered into the main belt [2]. No differentiation occurred for small planetesimals which formed in the asteroid belt as they formed too late to be melted.

However, this idea is currently motivated by the assumption that planetesimals can accrete faster closer to the sun due to an enhanced density of the nebula. While this is certainly true in general terms, this is probably not important for timescales of planetesimal formation. In a typical nebula and typical aggregation model planetesimal formation only needs 2000y at 1 AU [3]. Also cometesimals forming at 30AU from the sun do so quickly in less than 300.000y [3]. Both timescales are relatively short compared to the suggestion that the small difference of 1AU between the terrestrial planet region and the main asteroid belt should make a difference of 1 My in accretion. Therefore, some mechanisms are needed to delay planetesimal formation with respect to a typical aggregation model and trigger it somehow at a location moving slowly away from the sun.

**Inner edges of protoplanetary disks and photophoresis:** Recently a number of protoplanetary disks have been observed which clearly show evidence for a sharply truncated inner edge at several AU distance from their stars, TW Hya being one example [4]. Still gas is accreting in some of these objects [5]. This means that the inner clearing is mostly devoid of small dust and transparent to sunlight but the disks still contain significant amounts of gas. As outlined in our earlier work photophoresis inevitably acts on solid particles in such environments [6][7]. We find that photophoresis can push the inner edge outwards on timescales of 1My / 1AU and does not allow particles smaller than ~10cm to move inwards [8].

We suggest that photophoresis concentrated material at the inner edge of the Solar Nebula at an early stage leading to rapid accretion of asteroids and planetary embryos in the inner Solar System. Presence of <sup>26</sup>Al in these bodies caused all of these early accreted bodies to differentiate. Planetesimals continue to form as the edge moves outwards to the asteroid belt but at that time heating by <sup>26</sup>Al is no longer sufficient to differentiate these planetesimals.

**References:** [1] Bizarro M. et al. 2005. *Astrophysical Journal* 632:L41-L44. [2] Bottke W. F. et al. 2006. *Nature* 439:821-824. [3] Weidenschilling S. J. 2000. *Space Science Review* 92:281-296. [4] Calvet N. et al. 2002. *Astrophysical Journal* 568:1008-1016. [5] Rettig T. W. et al. 2004. *Astrophysical Journal* 616:L163-L166. [6] Krauss O. and Wurm G. 2005. *Astrophysical Journal* 630:1088-1092. [7] Wurm G. and Krauss O. 2006. *Icarus* 180:487-495. [8] Krauss O. and Wurm G. 2006. in preparation.

### HIGH-PRESSURE MINERAL ASSEMBLAGES IN SHOCK MELT VEINS OF SUIZHOU METEORITE

Xiande Xie<sup>1,2</sup>, Ming Chen<sup>2</sup> and Deqiang Wang<sup>2</sup>. <sup>1</sup>Guangdong Provincial Academy of Sciences, [xdxie@gzb.ac.cn](mailto:xdxie@gzb.ac.cn). <sup>2</sup>Guangzhou Institute of Geochemistry, Chinese Academy of Sciences.

The Suizhou meteorite was classified as a shock-vein-bearing L6 chondrite, and was evaluated by previous investigators as a weakly shock-metamorphosed (S2 to S3) meteorite. At the first glance, metal and troilite in Suizhou show almost no change (S2), and olivine and pyroxene show a few sets of shock-induced fractures (S2-S3)<sup>[1]</sup>, indicating that its shock stage of S2 to S3 was reasonable according to the principles of Stöffler's classification for shocked chondrites. However, our recent studies revealed that the Suizhou is an unique chondrite with specific and unusual shock-related mineralogical features: (1) Most of the plagioclase grains in the Suizhou unmelted chondritic rock were melted and transformed into maskelynite during the shock event, implying that plagioclase experienced strong compression (S5), and two morphological types of maskelynite were identified, namely, theomorphic and allomorphic maskelynites; (2) The very thin shock melt veins in Suizhou are filled with abundant various shock-produced high-pressure mineral phases, and no glassy phases have ever been identified in veins, indicating that this part of meteorite was very strongly shocked (S6); (3) The melt veins are consisted of two high-pressure mineral assemblages<sup>[1-8]</sup>: ① coarse-grained assemblage of minerals that occur as individual monomineralic or multiminerale grains, and it includes ringwoodite, majorite, akimotoite, devitrified perovskite, hollandite-structured NaAlSi<sub>3</sub>O<sub>8</sub>, tuite ( $\gamma$ -Ca<sub>3</sub>(PO<sub>4</sub>)<sub>2</sub>), and two post-spinel phases—the CaFe<sub>2</sub>O<sub>4</sub>- and CaTi<sub>2</sub>O<sub>4</sub>-type polymorphs of chromite; ② fine-grained mineral assemblage occurs as the matrix of the melt veins that has been totally crystallized into different mineral phases: idiomorphic garnet of majorite-pyrope composition (in solid solution), irregular magnesiowüstite and microcrystalline ringwoodite in interstices of garnet and magnesiowüstite grains. Therefore, the shock features listed above match a wide range of shock stages, namely, from S2 to S6, and hence, covered a wide range of shock-produced high pressures and temperatures from 5 to >45-90 GPa and 600 °C to 1750 °C. However, on the basis of our recent analyses, we come to a conclusion that the actual shock level of the Suizhou meteorite could be evaluated as S3-S4, and the unmelted chondritic rock of the meteorite experienced a shock pressure and temperature of up to 20~22 GPa and 1000 °C ~1100 °C, respectively. Locally developed thin shock melt veins in the meteorite were formed at the same or a bit higher pressure (up to 22~24 GPa) but at an elevated temperature of 2000°C~2200°C. The higher temperature in veins than that in unmelted chondritic rock was achieved by local shear-friction stress along the vein-stretching directions during the shock event.

**References:** [1] Xie X. et al. 2001. *European Journal of Mineralogy* 13:1177–1190. [2] Xie X. et al. 2001. *Chinese Science Bulletin* 46:1121–1126. [3] Xie X. et al. 2002. *Geochemica et Cosmochemica Acta* 66:2439–2444. [4] Xie X. et al. 2003. *European Journal of Mineralogy* 15:1001–1005. [5] Chen M. et al. 2004. *Meteoritics & Planetary Sciences* 39:1797–1808. [6] Chen M. et al. 2003. *Geochemica et Cosmochemica Acta* 67:3937–3942. [7] Chen M. et al. 2004. *Proceedings of National Academy of Science, USA* 100:14651–14654. [8] Xie X. et al. 2005. *Science in China, Series D* 48: 815–821.

## ALKALINE COPPER OXIDE DEGRADATION OF INSOLUBLE ORGANIC MATTER IN CARBONACEOUS CHONDRITES

H. Yabuta, G. D. Cody and C. M. O'D. Alexander. Carnegie Institution of Washington. E-mail: hyabuta@ciw.edu

**Introduction:** Recently, it has been revealed that hydrothermal treatment of insoluble organic matter (IOM) in CM chondrite markedly reduced oxygen-linked alkyl carbon components (O-CHx) then produced a variety of discrete organic molecules including prebiotic compounds such as dicarboxylic acids and benzimidazoles, as well as polycyclic aromatic hydrocarbons (PAHs) [1]. Comparative study of IOM structures in different types of chondrites [2] has also suggested that the partial conversion of O-CHx and CHx could have yielded some discrete organic molecules by aqueous alteration on the parent body. These results indicate that O-CHx in IOM could be a key structure in chemical evolution of chondritic organic matter during parent body processing. In this study, we have conducted alkaline CuO degradation of IOM for the purpose to elucidate the building blocks of the O-CHx structure and their abundances in molecular level by cleaving ether-linkages (C-O-C) in IOM selectively.

**Experimental:** The reaction of alkaline CuO degradation cleavages ether linkages of the molecule selectively and oxidizes the ether groups into carboxyl or hydroxyl groups [3]. A Teflon bomb (23ml) was loaded with 2 mg of Murchison IOM, 10 mg CuO powder, 1 mg of ammonium iron (II) sulfate hexahydrate  $[\text{Fe}(\text{NH}_4)_2(\text{SO}_4)_2 \cdot 6\text{H}_2\text{O}]$  and 2.5ml of 2M NaOH solution. The bomb was sealed and heated at 170°C for 3hrs. After the bomb had cooled down, the sample liquid was acidified to pH < 1, and extracted with ethyl acetate. The extract was dried under N<sub>2</sub> flow, derivatized with 100ul of N,O-bis-(trimethylsilyl) trifluoroacetamide (BSTFA) at 80°C for 3hrs, and analyzed by GC-MS.

**Results and Discussion:** Forty-seven compounds have been identified to date at 0.01 – 1 pmol/mg IOM level. They included 15 dicarboxylic acids (C<sub>2</sub> – C<sub>6</sub>), 11 hydroxy acids (C<sub>2</sub> – C<sub>6</sub>), 2 hydroxydicarboxylic acids (C<sub>4</sub>), 14 aromatic acids, and 5 other compounds. Among these compounds, all hydroxy- and hydroxydi- acids were seen for the first time as products of Alkaline CuO degradation of Murchison IOM, compared to the past study [3]. Succinic and benzoic acids were the most abundant (1.55 and 1.08 pmol /mg IOM, respectively). These results show that alkyl chains from C<sub>2</sub> to C<sub>7</sub> and one or two alkyl substituted aromatics (mainly benzene ring) were ether-linked in the IOM structure. Most of dicarboxylic, hydroxy- and hydroxydicarboxylic acids reported in this study have been identified from an aqueous extract of Murchison meteorite [4]. In addition, abundance of these acids declined with increasing carbon number, which is known to be a typical pattern for prebiotic synthesis of the compounds. These soluble acids in Murchison may be derived from the IOM during aqueous alteration. Residual IOM after oxidation was 60 – 75 % of the original weight, which were roughly consistent with aromaticity of Murchison IOM (61.7 – 65.7%) [2]. The residual portion is probably composed of aromatic and carbonyl carbons that were not reacted in the degradation.

**References:** [1] Yabuta H. et al. submitted. [2] Cody G. D. and Alexander C. M. O'D. 2005. *Geochimica Cosmochimica Acta* 69, pp. 1085-1097. [3] Hayatsu R et al. 1980. *Science* 207, 1202-1204. [4] Cronin J. R. et al. (1993) *Geochimica Cosmochimica Acta* 57, 4745-4752.

## MINERALOGICAL STUDY OF AUGITE-BEARING LODRANITE, NWA2235 AND IMPLICATION FOR ITS ORIGIN

A. Yamaguchi<sup>1</sup>, H. Takeda<sup>2</sup> and M. Kusakabe<sup>3</sup>. <sup>1</sup>National Institute of Polar Research, Tokyo 173-8515, Japan. E-mail: yamaguch@nipr.ac.jp. <sup>2</sup>Chiba Institute of Technology, Chiba 275-0016, Japan. <sup>3</sup>Institute for Study of the Earth's Interior, Okayama University, Misasa, Tottori 682-0913, Japan.

**Introduction:** Lodranites and acapulcoites belong to a subgroup of primitive achondrites, and possess recrystallized textures and modified chondritic mineralogy. The primitive achondrites experienced variable degrees of partial melting and melt migration. We performed a mineralogical study of a new augite-bearing lodranite, NWA2235. We examined a PTS of NWA2235 optically and with EPMA.

**Results:** The PTS of NWA2235 shows a coarse-grained aggregate with abundant 120° triple point junctures, composed of olivine (55 vol%) (Fa<sub>9.4-13.8</sub>), orthopyroxene (17%) (Ca<sub>2.0</sub>Mg<sub>46.1</sub>), augite (7%) (Ca<sub>44.3</sub>Mg<sub>50.5</sub>), FeNi metal (8.5%), troilite (1%), chromite, Ca-phosphates and weathering products. No plagioclase is observed in the PTS. Olivine grains contain small glass inclusions (~30-40 μm) rich in K<sub>2</sub>O and Na<sub>2</sub>O (~5-6 wt%). The grains of orthopyroxene (~4 mm) and augite (~2.6 mm) are very large, poikilitically enclosing surrounding minerals. Compositions of silicate minerals are within the ranges of lodranites and acapulcoites.

Although oxygen isotopic composition of NWA2235 ( $\delta^{17}\text{O}=1.62$ ,  $\delta^{18}\text{O}=4.94$ ) is slightly outside the range of lodranites, the  $\Delta^{17}\text{O}$  (= -0.96) is similar to those of common lodranites. Coupled with the textural and mineralogical data, we classified NWA2235 into a lodranite.

**Discussion:** Unlike other lodranites, NWA2235 contains large grains of augite and orthopyroxene. These pyroxene grains were likely formed during grain coarsening with minor amounts of melt [1]. The Na and K-rich glass inclusions in olivine could be trapped melt, indicating the presence of minor amount of partial melts. NWA2235 experienced a strong thermal metamorphism, minor melting and recrystallization.

Mineral abundances of lodranites vary significantly [2]. Different degrees of partial melting and melt migration (local segregation of partial melts), grain coarsening with minor amount of melts could explain the varying abundances. To explain the properties of lodranites, collisional heating has been suggested for the heat source for the metamorphism [1]. However, in the case of relatively small asteroids, impact heating is not effective heat source [3]. Yamaguchi et al. [4] suggested that moderate shock metamorphism at high temperatures near the solidus causes partial melting. We suggest that impacts occurred on the lodranite parent body which had been heated internally (e.g., by <sup>26</sup>Al). Different degrees of heating, brecciation and melting inside the parent body may explain the heterogeneous textures [1] of lodranites.

**References:** [1] Takeda H. et al. 1994. *Meteoritics* 29: 830-842. [2] Yugami K. et al. 1998. *Antarctic Meteorite Research* 11: 49-70. [3] McCoy T. et al. 1996. *Geochimica Cosmochimica Acta* 60: 2681-2708. [4] Yamaguchi A. et al. 2002. In *High-pressure shock compression of solids V*. p. 29-45.

**TEMPERATURE DEPENDENCE ON THE EFFECTS OF AQUEOUS ALTERATION ON MINERALOGY AND NOBLE GAS COMPOSITIONS IN CARBONACEOUS CHONDRITE NINGQIANG.**

Y. Yamamoto<sup>1</sup>, T. Nakamura<sup>2</sup>, T. Noguchi<sup>3</sup> and K. Nagao<sup>1</sup>.  
<sup>1</sup>Laboratory for Earthquake Chemistry, University of Tokyo, E-mail: y-yamam@eqchem.s.u-tokyo.ac.jp, <sup>2</sup>Department of Earth and Planetary Sciences, Kyushu University, <sup>3</sup>Department of Materials and Biological Science, Ibaraki University.

**Introduction:** Aqueous alteration is thought to be the earliest chemical reaction occurred in their parent bodies. Carbonaceous chondrites that experienced aqueous alteration might have changed mineralogy and noble gas compositions. In earlier work, we revealed that a major part of primordial noble gases in the Ningqiang carbonaceous chondrite lost during experimental aqueous alteration [1]. In order to understand the temperature dependence of mineralogical and noble gas compositional changes during aqueous alteration, we performed aqueous alteration experiments on Ningqiang at 100, 150, and 200°C. Powdered Ningqiang weighing 0.6g was kept in liquid water at these temperatures for 20 days. Mineralogy and noble gases in natural and altered Ningqiang were analyzed.

**Results and Discussion:** In the sample altered at 100°C, mineralogical changes are minor and could not be detected by XRD analyses. In contrast, 150 and 200°C altered samples greatly changed its mineralogical compositions. Olivine, low-Ca pyroxene and iron sulfide, which are main components of Ningqiang, were decomposed, and serpentine and hematite were formed. Serpentine appears to have formed from the elements supplied by the decomposition of olivine and pyroxene. It was confirmed by the electron microscopic observation that serpentine grown around olivine and pyroxene grains.

The aqueous alteration experiment also shows compositional change of trapped noble gases. The 100°C altered sample lost 6-20 % of trapped <sup>36</sup>Ar, <sup>84</sup>Kr and <sup>132</sup>Xe compared with those in natural Ningqiang. Significant depletions of trapped noble gases occurred at higher temperatures, i.e., 56-65 % and 83-94 % at 150 and 200°C, respectively. These results indicate that trapped Ar, Kr and Xe can be easily removed from their carrier phase in the temperature higher than 100°C. The (<sup>36</sup>Ar)<sub>trap</sub>/<sup>132</sup>Xe and <sup>84</sup>Kr/<sup>132</sup>Xe ratios in the 200°C altered sample were reduced to 85 and 1.2, respectively (natural Ningqiang: 235 and 1.4, respectively). Calculated (<sup>36</sup>Ar)<sub>trap</sub>/<sup>132</sup>Xe ratio of trapped noble gases removed through the alteration at 100°C is 68. Those in the sample altered at 150 and 200°C are 259 and 263, respectively. The (<sup>36</sup>Ar)<sub>trap</sub>/<sup>132</sup>Xe ratios removed at 150 and 200°C are higher than that in the 100°C sample and are in the range of Ar-rich gas in enstatite chondrites [2] and ureilites [3]. These results suggest that the Ar-rich gas in the Ningqiang is removed through the decomposition of olivine and pyroxene at temperatures higher than 100°C. Our results lead that both mineralogical and noble gas compositional changes by aqueous alteration are greatly dependent on its temperature.

**References:** [1] Yamamoto Y. et al. 2006. *Meteoritics & Planetary Science* 41:541-552. [2] Crabb J. and Anders E. 1981. *Geochimica et Cosmochimica Acta* 45:2443-2464. [3] Wacker J. F. 1986. *Geochimica et Cosmochimica Acta* 50:633-642.

## EVOLUTION OF DIFFERENTIATED ASTEROIDS AS INFERRED FROM COOLING RATES OF MAGMATIC IRON METEORITES.

J. Yang<sup>1</sup>, J. I. Goldstein<sup>1</sup> and E. R. D. Scott<sup>2</sup>. <sup>1</sup>Dept. of Mechanical and Industrial Engineering, University of Massachusetts, Amherst, MA 01003, USA. [jiyang@ecs.umass.edu](mailto:jiyang@ecs.umass.edu). <sup>2</sup>Hawai'i Institute of Geophysics and Planetary, University of Hawai'i, Honolulu, Hawai'i 96822, USA.

**Introduction:** Magmatic iron meteorites are generally thought to come from metallic cores of differentiated parent bodies that cooled slowly inside silicate mantles. Our new cooling rate data are incompatible with this model and imply that some cores and mantles were separated before the Widmanstätten pattern formed.

**Cooling Rates:** The metallographic cooling rates for both the IIIAB and IVA magmatic iron groups are correlated with bulk Ni content in each group [1, 2]. For IVA irons, cooling rates increase from 90 to 7000 K/Myr with decreasing Ni. For IIIAB irons, the cooling rate variation is smaller, 60-340 K/Myr. Even allowing for variations in nucleation mechanism and temperature, the cooling rate ranges in IIIAB and IVA are inconsistent with cooling in a core surrounded by a silicate mantle.

**Discussion:** The cooling rates of irons from the core of an asteroid with a silicate mantle should be the same [3]. Our cooling rates for the IIIAB and IVA irons are incompatible with such a model. We argue that their parent bodies experienced impacts that removed almost all of their silicate mantles before kamacite formed. For IIIAB irons, the impact produced a metallic core covered by some remaining silicate or regolith. For IVA irons, the impact left little or no silicate on the metallic core. Our cooling rate and thermal modeling suggest that at the time of the mantle-stripping impact, the temperature of the metallic core was 850-1200°C, i.e., the core and mantle may both have been partly molten. As a result, the metal cores then cooled faster near the surface and much slower near the center of the cores. If iron meteorites came from bodies that formed at 1-2 AU and were scattered into the asteroid belt by planetary embryos [4], the primary IVA and IIIAB bodies could have had their silicate mantles removed by tidal effects and impacts with embryos [5]. The very early separation of mantle materials from metallic cores may be the reason for the "missing" olivine meteorites [4].

Conventional thermal models imply that iron meteorite parent bodies had diameters of 24-130 km [6] or 4-200 km [7], but we infer that the metallic core of the IVA irons was around 300 km across and comparable in size to 16 Psyche, the largest known M class asteroid, which is 260 km across.

Our model also implies that the IIIAB and IVA cores crystallized inwards [8] not outwards [9] so high-Ni irons formed at the center.

**References:** [1] Yang J. and Goldstein J.I. 2006, *GCA*. In press. [2] Yang J. et al. 2006. *GCA*. To be submitted. [3] Haack H. et al. 1990. *JGR*. 95B:5111-5124. [4] Bottke et al. 2006. *Nature*. 439:821-824. [5] Asphaug E. et al. 2006. *Nature*. 439:155-160. [6] Haack H. and McCoy T. J. 2003. in *Meteorites, Comets and Planets*. Ed. by A.M. Davis. *Treatise on Geochemistry*. Vol.1. Elsevier, Amsterdam. 325-346. [7] Chabot N. L. and Haack H. 2006. in *Meteorites and the Early Solar System II*. In press. [8] Haack H and Scott E.R.D. 1992. *JGR*. 97:14727-14734. [9] Wasson J. T. 1985. *Meteorites: Their Record of Early Solar System History*. W.H. Freeman Press, New York.

**FRactal Dimension Analysis of Hellas Basin:  
The Martian Impact Crater Might Be Ancient  
Lakes/Seas**

Guo Yangrui<sup>1</sup> Taiyuan No.5 High School, China E-mail:  
G2COM@126.com

**Introduction:** Some Martian impact craters are considered as ancient lakes or seas, e.g., Hellas and Rabe. Parker proposed the Martian shoreline in Northern Plain in 1989, and the shoreline has two different levels [6], [7]. It aroused many controversies on whether the early Mars had oceans and the topography was formed by wave or wind. Fractal analysis allows quantification of natural objects that appear to be in a statistical scene self-similarity. Bernard Sapoval pointed out wave erosion was main power to form coastline fractal. [3] Terrestrial coastlines show dimensions between 1.13 and 1.25. [1], [2] Wind erosion is non-fractal, which has fewer dimensions. This study proposed fractal method in order to analyze erosion process in Hellas.

Hellas impact basin is one of the most prominent topographic features in the southern hemisphere of Mars. Hellas basin is about nine kilometers deep. The main basin rim is about 2300 km in diameter. Below -5800m large impact craters are not apparent in Hellas, between -5800 and -1800m large craters are present but are degraded [4], [5]. I used U.S. Geological Survey Mars Global Digital Elevation Model, based on Mars Orbiter Laser Altimeter data at scale 1:10,000,000, clipped out the Hellas region. The contours at elevations -3000m, -3500m, -4000m, -4500m, -5000m, -5500m and two proposed shorelines at elevations -3100m and -5800m were drawn automatically using a geographic information system (GIS) software package. All contours are closed-curves. An image-processing program HarFa 5.1 via Box-counting method calculated the fractal dimensions. The fractal dimension is the slope of the straight line Black & White. The 8 results show a fractal dimensions ranging from 1.147 to 1.235, and mean is 1.182.

**Conclusions:** The contours are fractal, so the topography must be created by fractal geologic process. If the topography were formed by wave erosion, they might keep some original features. Therefore, the result of analyze of Hellas shoreline/lakeshore fall within terrestrial results that can be interpreted as strong evidence of Hellas as a lake/sea on Mars. Scientists used rules of thumb in order to deduce climate on early Mars. The fractal analysis can provide a new way for understanding Martian histories. As the water in Hellas slowly disappeared, the sea level decreased and wave actions continued, so all the results could be kept in a certain range. Water decelerated and prevented small meteorites from falling into Hellas. The degraded impact craters might be eroded by wave actions; some small-integrated craters might be formed after the water disappeared.

**Main References:** [1] S.C.Cull.2003. Abstract #1100. 34<sup>th</sup> Lunar & Planetary Science Conference. [2] B. B. Mandelbrot. 1967. *Science* 156:636-638 [3] B. Sapoval et al. 2004. Abstract #NG11A-06.2004 JOINT ASSEMBLY. [4] David A. Crown et al.2005. Abstract#2097.36<sup>th</sup> Lunar & Planetary Science Conference. [5] J. M. Moore. et al. 2001. Abstract #1446.32<sup>nd</sup> Lunar and Planetary Science [6] Parker, T.J., et al., 1989, *Icarus* 82, 111-145. [7] Carr, M. H. and Head III, J. W. 2003. *Journal of Geophysical Research*, Volume 108, Issue E5, pp. 8-1.

### SUPERNOVA MIXTURES REPRODUCING ISOTOPIC RATIOS OF LOW DENSITY GRAPHITE GRAINS.

T. Yoshida. National Astronomical Observatory of Japan, Tokyo 181-8588, Japan. E-mail: takashi.yoshida@nao.ac.jp.

**Introduction:** Low density graphite grains are believed to be originating from supernovae [1]. They have excesses of  $^{28}\text{Si}$  and  $^{18}\text{O}$ , and some of them have evidence for the original presence of  $^{44}\text{Ti}$  [1,2]. Recently, their isotopic ratios have been compared quantitatively with those deduced from supernova nucleosynthesis calculations [3,4]. In order to reproduce the isotopic and elemental signatures, large-scale heterogeneous mixing of supernova ejecta should be taken into account. In this study, we seek mixtures of supernova ejecta reproducing isotopic ratios of low density graphite grains. We also investigate the mixing ratios and compositions of the mixtures.

**Supernova Mixing Models:** We use the abundance distributions of the supernova ejecta of 3.3, 4, 6, and 8  $M_{\text{solar}}$  He star models corresponding to 13, 15, 20, and 25  $M_{\text{solar}}$  zero-age main sequence stars [4]. We divide the supernova ejecta into seven layers; the Ni, Si/S, O/Si, O/Ne, C/O or O/C, He/C, and He/N layers. Then, we seek mixtures reproducing  $N_{\text{iso}}$  isotopic ratios of individual graphite grains using  $\chi^2$ -value evaluation. We seek the minimum  $\chi^2$ -value and the corresponding mixing ratios. When the  $\chi^2$ -value of a mixture corresponding to a grain is smaller than  $4N_{\text{iso}}$ , we consider that the mixture reproduces  $N_{\text{iso}}$  isotopic ratios of the grain.

**Results:** We pick up 26 low density graphite grains in [3] and seek mixtures reproducing  $^{12}\text{C}/^{13}\text{C}$ ,  $^{14}\text{N}/^{15}\text{N}$ ,  $^{16}\text{O}/^{17}\text{O}$ ,  $^{16}\text{O}/^{18}\text{O}$ ,  $^{26}\text{Al}/^{27}\text{Al}$ ,  $^{29}\text{Si}/^{28}\text{Si}$ , and  $^{30}\text{Si}/^{28}\text{Si}$  of the individual grains. For three grains,  $^{44}\text{Ti}/^{48}\text{Ti}$  is also compared. We find mixtures reproducing six isotopic ratios for 20 individual graphite grains. The mixtures are classified into three groups. The mixtures in the first group reproduce the isotopic ratios except  $^{14}\text{N}/^{15}\text{N}$ . The main component of the mixtures is the He/N layer. Most of the mixtures indicate the mixing ratios of the He/N layer larger than 0.8. The mixtures also indicate  $^{14}\text{N}/^{15}\text{N}$  much larger than the measured one. The mixtures in the second group reproduce the isotopic ratios except  $^{12}\text{C}/^{13}\text{C}$ , which is much larger than the measured ratios. The main component is the He/C layer so that  $^{14}\text{N}/^{15}\text{N}$  and the excesses of  $^{18}\text{O}$  in the grains are well reproduced. The second main component is the He/N layer and its mixing ratio is of order 0.1 in most cases. The mixtures in the third group reproduce both  $^{12}\text{C}/^{13}\text{C}$  and  $^{14}\text{N}/^{15}\text{N}$  but show large  $^{26}\text{Al}/^{27}\text{Al}$ . The main component is the Ni layer; the mixing ratio is larger than 0.9 for most cases. For one grain of which  $^{44}\text{Ti}/^{48}\text{Ti}$  has been measured, we find mixtures reproducing six isotopic ratios including  $^{44}\text{Ti}/^{48}\text{Ti}$ . The mixing ratios of the mixtures are similar to those in the first group. The C/O ratios in most of the mixtures are larger than unity. Elemental composition of the mixtures will be constrained by the formation theory of presolar grains from supernovae.

**References:** [1] Amari S., Zinner E., and Lewis R. S. 1995. *Astrophys. J. Lett.* 447: L147-L150. [2] Nitter L. R. et al. 1996. *Astrophys. J. Lett.* 462: L31-L34. [3] Travaglio et al. 1999. *Astrophys. J.* 510: 325-354. [4] Yoshida T., Umeda H., and Nomoto K. 2005. *Astrophys. J.* 631: 1039-1050.

### O-ISOTOPIC DISTRIBUTION OF PORPHYRITIC AND NON-PORPHYRITIC CHONDRULES IN ACFER 214, CH CHONDRITE.

M. Yoshitake<sup>1</sup> and H. Yurimoto<sup>2</sup>, <sup>1</sup>Department of Earth and Planetary Sciences, Kobe University, 1-1 Rokkoudai-cho, Nada, Kobe 657-8501, Japan. E-mail: miwa@kobe-u.ac.jp. <sup>2</sup>Natural History Sciences, Hokkaido University, Sapporo 060-0810, Japan.

**Introduction:** Chondrules are one of the major components in chondrites. Clayton et al. [1] reported that O-isotopic compositions of 23 chondrules in the Allende meteorite. Porphyritic type chondrules have more <sup>16</sup>O-rich compositions than barred olivine chondrules in the Allende meteorite. These O-isotopic distributions can be explained by interaction between a solid precursor (<sup>16</sup>O-rich) and a nebular gas (<sup>16</sup>O-poor) during the chondrule-forming events [1, 2]. The range and frequency of the distribution reflect the degree of equilibrium of the exchange or O-isotopic composition of nebula gas at chondrule fraction.

On the other hand, previous study revealed that a CH chondrite contains a chondrule extremely enriched in <sup>16</sup>O [3]. This result suggests that chondrules in CH chondrites may retain its original O-isotopic composition.

**Results and Discussion:** We identified chondrules in Acfer 214 CH chondrite, and classified into porphyritic olivine (PO, 19.2%), porphyritic olivine pyroxene (POP, 25.8%), porphyritic pyroxene (PP, 4.6%), granular olivine pyroxene (GOP, 3.3%), cryptocrystalline (C, 37.1%), and barred olivine (BO, 9.9%) chondrules by backscattered electron images using SEM-EDS. Oxygen isotopic compositions in 151 chondrules of the Acfer 214 chondrite were analyzed by secondary ion mass spectrometry using the CAMECA ims 1270.

All O-isotopic compositions of chondrules were plotted along the CCAM line. The O-isotopic compositions in these chondrules distributed from -20 to +15‰ ( $\delta^{18}\text{O}$ ) except a chondrule reported by [3]. This is consistent with previous reports [3, 4, 5]. These results indicate that O-isotopic distribution of chondrules in CH chondrite is wider than that of Allende [1, 2]. Moreover, O-isotopic compositions of non-porphyritic (C and BO) chondrules distributed from -19 to +12‰ ( $\delta^{18}\text{O}$ ). This distribution is wider than that of porphyritic type (PO, PP, POP, and GOP) chondrules. This trend of O-isotopic compositions between non-porphyritic and porphyritic types chondrules differs from the case of Allende meteorite [2, 6]. In this case, O-isotopic exchange process was not caused O-isotopic compositions of chondrules in Acfer 214. These results indicate that chondrule precursors had different O-isotopic compositions one another or chondrule formation occurred in various environments with different O-isotopic compositions.

**References**[1] Clayton R. N. et al. 1983. In *Chondrule and Their Origins*, 37-43. [2] McSween H. Y. Jr. 1985. *Meteoritics*, 20: 523-540. [3] Kobayashi S. et al. 2003. *Geochem. J.*, 37: 663-669 [4] Krot A. N. et al. 2000. Abstract #1459. 31st Lunar & Planetary Science Conference. [5] Jones et al. 2005. Abstract #1813. 36th Lunar & Planetary Science Conference. [6] Clayton R. N. et al. 1993. *Annu. Rev. Earth & Planet. Sci.* 21: 115-149.

**POSSIBLE HEIGHTENED NOCTILUCENT CLOUD ACTIVITY NEAR STRONG PERSEID MAXIMA.**

M. Zalcik<sup>1</sup>, A. A. Mardon<sup>2</sup>, <sup>1</sup>Noctilucent Cloud Canadian-American Network ([bluegrama@shaw.ca](mailto:bluegrama@shaw.ca)), <sup>2</sup>Antarctic Institute of Canada (PO Box 1223, MPO, Edmonton, AB, Canada T5J 2M4. [amardon@shaw.ca](mailto:amardon@shaw.ca)),

**Introduction:** Noctilucent clouds (NLC) are ice clouds that form in Earth's mesosphere at heights of 80-85km[1]. The accretion nuclei of NLC are thought to include meteoric particles as well as hydrated ions[2]. It has been argued that significant intrusions of meteor dust resulting from major meteoric events could increase the availability of nuclei, rendering more and/or brighter displays, the most compelling example being a bright display of NLC immediately following the Tunguska, Russia (60.9N 101.9E), fireball of 30 June 1908[3]. To see if heightened activity by the Perseid meteor shower in 2004 as reported by the International Meteor Organization[4] and predicted by P. Brown[5] had any effect on NLC during the Perseid peak dates of Aug 11-12, we examined NLC observations at the Rankin Inlet, Canada, NU Flight Service Station (62.4N 92.1W) and the Baker Lake, Canada NU Community Aerodrome Radio Station (64.2N 96.1W), participants in the NLC CAN AM NLC observing network. *Table #1* lists the results for the years 2003 to 2005 inclusive. There were two nights with NLC in 2004 as seen from Baker Lake, but, compared with the other years in the study, there does not seem to have been a substantial increase in activity around the dates of the Perseid peak. The inherent interference by tropospheric clouds, which prevent (the farther away) NLC from being seen, makes any conclusions somewhat shaky. Indeed, of the six sightings listed in the *Table # 1*, only two of these were made under ideal tropospheric conditions themselves.

*Table #1:* Comparison of Perseid Peak dates from two years compared with observations of Noctilucent Clouds in two Northern Canadian NLC CAN AM NLC observing sites in 2003, 2004 & 2005.

	Rankin Inlet, Canada				Baker Lake, Canada			
	Aug 10/11	11/12	12/13	13/14	Aug 10/11	11/12	12/13	13/14
2003	---	---	---	Y	---	Y	---	Y
2004	---	---	---	---	Y	---	---	Y
2005	---	Y	---	---	---	---	---	---

Y - yes, NLC seen; --- - interference by tropospheric clouds

**Conclusion:** NLC activity as seen from Rankin Inlet, NU and Baker Lake, NU around the time of the strong Perseid meteor shower peak in 2004 was no higher than NLC activity at the same sites and dates in 2003 and 2005. Hence, perhaps a higher flux of shower meteors does not render heightened NLC activity. Interference by tropospheric clouds at both sites makes any conclusions difficult to support.

**References:** [1] Gadsden, M., Schroeder, W. (1989), *Noctilucent Clouds*, Springer Verlag. [2] Turco, R.P., Toon, O.B., Whitten, R.C., Keesee, R.G., Hollenback, D. (1982) "Noctilucent clouds: simulation studies of their genesis, properties, and global influences." *Planetary and Space Science* 30: 1147-1181. [3] Vestine, E.H. (1934) "Noctilucent clouds." *Journal of the Royal Astronomical Society of Canada* 28: 249-272, 303-317. [4] International Meteor Organization (2004) [www.imo.net/news/perseids2004-4](http://www.imo.net/news/perseids2004-4). [5] Brown, P. (2006) Personal Communication, Canada.

### SOME APPLICATIONS OF THE CHONDRITE OXYGEN MIXING MODEL

B. Zanda<sup>1,2</sup>, R. H. Hewins<sup>2</sup>. <sup>1</sup>MNHN-CNRS UMS2679, 75005 - Paris. E-mail: zanda@mnhn.fr. <sup>2</sup>Geological Sciences, Rutgers University, Piscataway NJ08855.

**Introduction:** Abundances of the petrographic constituents of chondrites (type I and type II chondrules, refractory inclusions, metal and matrix) correlate within chondrite groups, indicating that these groups were generated by the mixing of a limited number of simple reservoirs, hereafter called “primary mixes” [1]. The abundances of petrographic constituents also correlate with oxygen isotope signatures across chondrite groups and this allowed us to extract the oxygen isotopic signatures associated with the five petrographic constituent pure poles at the time of isolation of the chondritic reservoirs [2].

**Applications:** *Oxygen isotopic signatures of chondrite classes.* Based on those of the pure poles, we derived the oxygen isotopic signatures associated to the primary mixes: these allow to precisely describe the oxygen isotopic signatures of all the chondrites groups. For example, CM and CO chondrites are known to lie on a slope 0.7 line in the 3-isotope plot [3] which is very accurately predicted by this model.

*Other mixing trends.* Other mixing trends appear obvious in the oxygen 3-isotope plot. For example, pallasites lie on a 1.3 slope line in the 3-isotope plot with  $R^2=0.99$ , a trend unexplained so far, but on which some light can be shed from the primary mixes lying close to the end-members of the trend.

*Chemical and petrological information.* The C concentration of chondrites exhibits a weak correlation with their matrix abundance. The correlation between C concentration and  $\Delta_{18}O$  is much stronger because  $\Delta_{18}O$  is actually a more integrative measurement of matrix abundance in a chondrite than measurements done by point counting. As various achondrites also plot on the C vs  $\Delta_{18}O$  correlation, this indicates that they initially contained matrix similar to that of chondrites and allows to derive the abundance of that matrix

**Conclusion:** The chondrite oxygen mixing model is a powerful tool which allows to understand the relationship between all the chondrite groups. Applied to primitive achondrites and differentiated meteorites it can be used to make inferences on their initial petrography and chemistry.

**References:** [1] Zanda B. and Hewins R.H. (2006) Lunar Planet. Sci. XXXVII #2199. [2] Zanda B. et al. (2006) Earth Planet. Sci. Lett., in press. [3] Clayton R.N. (2005) Treatise of Geochemistry I, 129-142.

### COORDINATED STRUCTURE-ISOTOPE STUDIES OF PRESOLAR HIBONITES.

T. J. Zega<sup>1</sup>, R. M. Stroud<sup>1</sup>, L. R. Nittler<sup>2</sup>, and C. M. O'D. Alexander<sup>2</sup> <sup>1</sup>Naval Research Laboratory, Code 6360, 4555 Overlook Ave. SW, Washington D.C., 20375. <sup>2</sup>Department of Terrestrial Magnetism, Carnegie Institution of Washington, 5241 Broad Branch Rd NW, Washington DC, 20015. (zega@nrl.navy.mil).

**Introduction:** Hibonite ( $\text{CaAl}_{12}\text{O}_{19}$ , S.G.:  $P6_3/mmc$ ) is predicted to be the second major oxide to condense from a gas of solar composition [1]. It is a major constituent of calcium- and aluminum-rich inclusions in chondritic meteorites, and it has been identified in the infrared spectra of planetary nebulae [2]. Thus, information on the structure and composition of hibonite is important for constraining the conditions of circumstellar environments and providing ground-truth for observational astronomy. [3] used transmission electron microscopy to provide the first structural confirmation and characterization of presolar hibonite. Here we expand on those efforts and report results from two additional grains.

**Methods:** An acid-residue of Krymka meteorite was analyzed using a Cameca IMS 6f and nanoSIMS 50 secondary ion microprobes (SIMS), and the presolar grains were identified on the basis of their O isotope values [4]. We used the focused-ion-beam scanning-electron microscope (FIB-SEM) to create, thin, and extract, in situ, electron-transparent sections [5] for further investigation with a transmission electron microscope (TEM). The FIB section was analyzed using a 200 keV JEOL 2200FS TEM equipped with an energy-dispersive spectrometer, in-column energy filter, and bright- and dark-field detectors.

**Results and Discussion:** SIMS analysis reveals that both grains are  $^{18}\text{O}$  depleted and fall in the Group 2 category for presolar oxides, suggesting that they formed in low-mass asymptotic giant branch stars that experienced cool-bottom processing [6]. Grain KR-1-83-2 has  $\delta^{17}\text{O} = 722 \pm 30\text{‰}$  and  $\delta^{18}\text{O} = -888 \pm 19\text{‰}$ , whereas grain KR3B-92-11 has  $\delta^{17}\text{O} = 2064 \pm 95\text{‰}$  and  $\delta^{18}\text{O} = -768 \pm 8\text{‰}$ .

Measurements on selected-area electron-diffraction patterns acquired from the grains confirm the identity and crystallinity of the hibonite. TEM bright-field and high-angle annular-dark-field imaging reveals that both grains have uniform contrast, verifying that they are single crystalline with no evidence of subgrains. High-resolution TEM imaging on KR1-83-2 reveals that lattice fringes are discontinuous in some areas, suggesting minor amorphization, possibly due to pre-accretionary radiation processing. Energy-dispersive spectroscopy shows that grain KR1-83-2 contains abundant Al and Ca with minor Ti and Fe, whereas grain KR3B-92-11 contains abundant Al, Ca, Ti, and minor Mg. These results are generally consistent with equilibrium condensation predictions and the previous report by [3] of a Group 1 hibonite grain.

**References:** [1] Lodders K. 2003. *The Astrophysical Journal* 591: 1220-1247. [2] Hofmeister A. M. et al. 2004. *Geochimica et Cosmochimica Acta* 68:4485-4503. [3] Stroud R. M. et al. 2005. *Meteoritics and Planetary Science* 40:A148. [4] Nittler L. R. et al. 2005. Abstract #2200. 36<sup>th</sup> Lunar and Planetary Science Conference. [5] Zega T. J. and Stroud R. M. 2006. Abstract #1441 37<sup>th</sup> Lunar and Planetary Science Conference. [6] Wasserburg G. J. et al. 1995. *Astrophysical Journal Letters* 447:L37-40.

**PAIRING AND PETROGENETIC RELATIONSHIPS AMONG BASALTIC LUNAR METEORITES FROM NORTHWEST AFRICA.** R.A. Zeigler<sup>1</sup>, R. L. Korotev<sup>1</sup>, B. L. Jolliff<sup>1</sup>, T. E. Bunch<sup>2</sup>, and A. J. Irving<sup>3</sup>, <sup>1</sup>Dept. Earth & Planetary Sciences, Washington University, Campus Box 1169, St. Louis, MO 63130 zeigler@levee.wustl.edu <sup>2</sup> Dept. of Geology, Northern Arizona University, Flagstaff, AZ 86011. <sup>3</sup>Dept. Earth & Space Sciences, University of Washington, Seattle, WA 98195.

Several lunar meteorite stones discovered in northwestern Africa since 2000 are fragments of a single, complex, coarse-grained basaltic breccia from the Moon. The stones, about 1.2 kg in total mass, include previously studied NWA (Northwest Africa) 773 [1,2] and more recently discovered NWA 2700, NWA 2727, NWA 2977, NWA 3160 [3,4], and at least one other yet-to-be described stone.

As a whole, the meteorite consists of several lithologies, but the breccia is sufficiently coarse grained and the stones sufficiently small that individual stones each contain only a subset of the lithologies. The meteorite is best described as a fragmental breccia consisting mainly of clasts, some greater than 1 cm in size, of porphyritic olivine basalt, (most prominent in stones 2727 and 3160) and cumulate olivine gabbro (most prominent in 773, 2700, and 2977) [1]. NWA 773 also contains regolith breccia that is finer grained than the fragmental breccia and which itself contains a minor component of nonmare material [1,2]. NWA 2727 contains a minor component of ferrogabbro [4].

We conclude that the stones are paired on the basis of their compositional and textural similarity to each other and their uniqueness as whole compared to other lunar samples. The olivine basalt is a VLT (very-low-Ti) lunar basalt [1]. On the basis of mineral composition and bulk sample composition (INAA [5]), the same basalt occurs in all the stones. Similarly, the olivine cumulate is compositionally distinct. Both lithologies share several key trace-element characteristics that show they are petrogenetically related to each other and together distinct from any other basaltic lunar meteorite and any basalt from the Apollo and Luna collection. These features are relative enrichment in LREE, high Th/REE, and very low concentrations of the 'plagiophile' elements Na<sub>2</sub>O, Sr, and Eu. This fingerprint suggests a common source region for the different lithologies, one that is different from that of nearly any previously studied lunar basalt.

For NWA 773, Jolliff et al. [2] argued for a shallow intrusive setting for crystallization of the olivine cumulate and derivation from a melt of composition similar to Apollo 14 VLT volcanic glass, with modest assimilation of a KREEP component. Moreover, the breccia associated with the olivine cumulate may be dominated by extrusive VLT basalt related to the shallow intrusive. We will test this and other scenarios for petrogenetic relationships using data from the new NWA meteorites

**References:** [1] Fagan T. J. et al. (2003) *MAPS* **38**: 529-554. [2] Jolliff B. L. et al. (2003) *GCA* **67**: 4857-4879. [3] Zeigler R. A., et al. (2006) *LPS XXXVII*, Abstract #1804. [4] Bunch T. E. et al. (2006) *LPS XXXVII*, Abstract #1375. [5] Zeigler et al. (2006) *Antarctic Meteorites XXX*. **Acknowledgements:** This work was supported by NASA grant NNG04GG10G.

## PETROGRAPHIC AND MINERALOGICAL STUDIES OF THE LUNAR METEORITE DHOFAR 1180

Aicheng Zhang and Weibiao Hsu. Purple Mountain Observatory, Nanjing, 210008, China. E-mail: aczhang@pmo.ac.cn.

**Introduction:** Lunar meteorites provide important clues to better understand the formation and evolution of the Moon. Up to now, near 40 lunar meteorites were identified, and most were found in cold- and hot-deserts [1]. Dhofar 1180 is a newly recovered lunar breccia from Oman in 2005. Here, we present petrographic and mineralogical studies of this new lunar meteorite.

**Results:** Dhofar 1180 is a polymict breccia that contains lithic clasts of gabbro, anorthositic gabbro, granulite, subophitic basalt, troctolite, Ti-rich clast (olivine and pyroxene grains set in Ti-rich glass), microporphyritic crystalline impact melt breccia and gabbroic anorthosite. They usually occur as angular fragments ranging in size from 0.1 to 1 mm. Individual mineral fragments of pyroxenes, olivine and anorthite are abundant in the matrix, as well impact glass with various sizes. They range in size from 0.1 to 1 mm. Some pyroxene grains display fine exsolution. Most large mineral fragments show undulose extinction.

Mineral chemistry varies from clast to clast. Olivine usually has a Fa value of 31 to 69. In the Ti-rich clast, the value in olivine varies from 54 to 98. For olivine grains with MnO > 0.10 wt%, the molar FeO/MnO ratio varies from 70 - 110 with an average of 93, which falls within the range of typical lunar olivines [2]. Pyroxene also shows extensive chemical variation among clasts. Pyroxene mainly occurs as pigeonite ( $\text{En}_{24-66}\text{Fs}_{23-59}\text{Wo}_{6-24}$ ), augite ( $\text{En}_{11-41}\text{Fs}_{23-59}\text{Wo}_{28-38}$ ), and pyroxferroite ( $\text{En}_{1-9}\text{Fs}_{65-86}\text{Wo}_{14-26}$ ). The molar FeO/MnO ratio of pyroxene varies from 50 to 70 with an average of 63. Anorthite is highly enriched in Ca and shows a small compositional variation ( $\text{An}_{91-99}$ ) among clasts. Chromite-spinel-ulvospinel solid solution and ilmenite were also found in clasts. The impact glass has a composition of anorthite and contains several per cents of MgO and FeO.

**Discussion:** Whole rock compositions of Dhofar 1180 bear many characteristics of lunar meteorites [3]. It was classified as a fragmental or regolith breccia. Petrography and mineral chemistry of plagioclase, olivine and pyroxene are consistent with a lunar origin [4, 5]. The existences of anorthositic clasts and pyroxferroite further confirm the conclusion.

Among well-defined lunar meteorites, Dhofar 1180 has  $\text{Al}_2\text{O}_3$  (23 wt%) and FeO (9.2 wt%) contents similar to those of Yamato 983885 and Calcalong Creek [1,3]. However, its Th concentration (0.9 ppm) is significantly lower than that of Yamato 983885 (2 ppm) and Calcalong Creek (4 ppm) [3]. Our data shows that KREEP basalt that occurred in both Yamato 983885 and Calcalong Creek is absent in Dhofar 1180. In Dhofar 1180, Ti-rich clast and impact glass are abundant, but are absent in Yamato 983885 and Calcalong Creek although low-Ti basalt clast was reported in Calcalong Creek [4,6]. The above distinction among Dhofar 1180, Yamato 983885 and Calcalong Creek suggests that Dhofar 1180 probably represent a unique lunar breccia.

**References:** [1] Korotev R. L. 2005. *Chemie der Erde* 65, 297-346. [2] Papike J. J. 1998. *Review in Mineralogy* V36. [3] [http://epsc.wustl.edu/admin/resources/moon\\_meteorites.html](http://epsc.wustl.edu/admin/resources/moon_meteorites.html). [4] Arai T. et al. 2005. *Antarctic Meteorite Research* 18, 17-45. [5] Kaiden H. and Kojima H. 2002. Abstract #1598. XXXIII LPSC. [6] Hill D. H. and Boynton W. V. 2003. *Meteoritics & Planetary Science* 38, 595-626.

### STUDY OF METAL EXTRACTED FROM TZAREV L5 CHONDRITE BY MÖSSBAUER SPECTROSCOPY AND METALLOGRAPHY

E.V. Zhiganova and M.I. Oshtrakh. Faculty of Physical Techniques and Devices for Quality Control, Ural State Technical University – UPI, Ekaterinburg, 620002, Russian Federation.  
E-Mail: evgeniya@dpt.ustu.ru, oshtrakh@mail.utmet.ru

**Introduction:** Mössbauer spectra of ordinary chondrites consist of several components related to metal, troilite, olivine, pyroxene and iron oxides. The area of metal subpeaks does not exceed 20 % and this value is related to the metal iron content. Usually chondrite metal contains more than one metal phase but they cannot be resolved in complicated Mössbauer spectrum of chondrite sample [1, 2]. Therefore, metal extraction from meteorite matter is necessary for detailed study by Mössbauer spectroscopy.

**Methods:** Sample of metal extracted from ordinary chondrite Tzarev L5 was prepared as powder and glued on pure aluminum foil. Extraction was performed by several steps: powdering, levigation in acetone followed by the separation in strong and weak magnetic fields, then drying and etching by weak HF, and final selection with binocular loupe from silicates. Mössbauer spectrum was measured at room temperature using spectrometer SM-2201 with high accuracy, stability and sensitivity in transmission geometry with moving absorber. Sections of Tzarev L5 for metallography were polished with diamond paste and etched by Nital (2 vol. %  $\text{HNO}_3$ , balance ethyl alcohol). Chemical composition of metal was obtained by microanalysis EDAX realized on SEM.

**Results:** Mössbauer spectrum of metal from Tzarev L5 was measured with high velocity resolution using 4096 channels and then presented in 1024 channels for fitting (see Fig. 1, A). The results of the spectrum better fit demonstrated the presence of 3 sextets with the hyperfine field values related to kamacite  $\alpha$ -Fe(Ni,Co), martensite  $\alpha_2$ -Fe(Ni,Co) and kamacite  $\alpha'$ -Fe(Ni,Co), one doublet related to residue olivine, and one singlet related to taenite  $\gamma$ -Fe(Ni,Co). The result of the metal grains metallography is shown in Fig. 1, B and demonstrates the presence of various metal phases:  $\alpha$ -Fe(Ni,Co) (1),  $\alpha_2$ -Fe(Ni,Co) (2), and both  $\alpha'$ -Fe(Ni,Co) (3) and  $\gamma$ -Fe(Ni,Co) (4) in plessite.

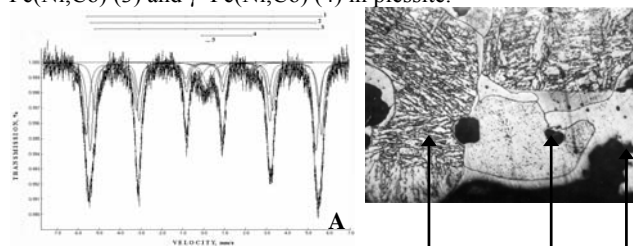


**Fig.1.** A – Mössbauer spectrum of metal extracted from Tzarev L5 (1–3, 5 are metal components, 4 is residue olivine), T=295 K; B – Microphotograph of the metal grain in Tzarev L5.

**Conclusion:** Study of extracted metal from Tzarev L5 by Mössbauer spectroscopy permitted us to reveal 4 different metal phases and determine its hyperfine parameters and relative areas. These results were in good agreement with metallography data.

**References:** [1] E.V. Zhiganova et al. 2005 *Meteoritics&Planetary Science*, 40:A174. [2] E.V. Zhiganova et al. *Hyperfine Interact.*, submitted.

### Si AND C ISOTOPIC RATIOS IN AGB STARS: SiC GRAIN DATA, MODELS, AND THE GALACTIC EVOLUTION OF THE Si ISOTOPES.

E. Zinner<sup>1</sup>, L. R. Nittler<sup>2</sup>, R. Gallino<sup>3,7</sup>, A. I. Karakas<sup>4</sup>, M. Lugaro<sup>5</sup>, O. Straniero<sup>6</sup>, J. C. Lattanzio<sup>7</sup>. <sup>1</sup>Washington University, St. Louis, MO 63130, USA, [ekz@wustl.edu](mailto:ekz@wustl.edu). <sup>2</sup>Carnegie Institution of Washington, NW Washington DC, 20015, USA. <sup>3</sup>Università di Torino, Italy. <sup>4</sup>McMaster University, Hamilton, ON, L8S 4M1, Canada. <sup>5</sup>University of Utrecht, 3508 TA Utrecht, The Netherlands. <sup>6</sup>INAF, Osservatorio Astronomico di Teramo, Italy. <sup>7</sup>Monash University, Victoria 3800, Australia.

Presolar grains of the mainstream, Y and Z type are believed to have an origin in carbon stars. We compared the C and Si isotopic ratios of these grains [1] with the results of theoretical models for the envelope compositions of AGB stars. Two sets of models (FRANEC, Monash) use a range of stellar masses (1.5 to 5M<sub>⊙</sub>), metallicities, different prescriptions for mass loss, and two sets of neutron-capture cross sections for the Si isotopes [2, 3]. They predict that the shifts in Si isotopic ratios and the increase of <sup>12</sup>C/<sup>13</sup>C in the envelope during third dredge-up are higher for higher stellar mass, lower metallicity, and lower mass loss rate. The Guber et al. [3] cross sections result in larger shift in the <sup>30</sup>Si/<sup>28</sup>Si ratios and smaller shifts in the <sup>29</sup>Si/<sup>28</sup>Si ratios than the Bao et al. [2] cross sections. Because the <sup>22</sup>Ne neutron source dominates Si nucleosynthesis, the effect of the <sup>13</sup>C source is negligible.

Comparison of the model predictions with grain data confirms an AGB origin for mainstream, Y, and Z grains, with the first type coming from stars with solar metallicity [4], the rest from stars with lower-than-solar metallicity [1, 5, 6]. The Si isotopic ratios of the Z grains favor the more recent Guber et al. [3] cross sections. The <sup>12</sup>C/<sup>13</sup>C ratios of low-metallicity models are much higher than those found in Z grains and cool bottom processing [7] must be invoked to explain the grains' C isotopic ratios. The high predicted C/O ratios in low-metallicity stars not experiencing this process might have prevented the formation of SiC and led to the condensation of graphite instead [8]. By combining Z grain Si data with the models we determined the evolution of the <sup>29</sup>Si/<sup>28</sup>Si ratios in the Galaxy as function of metallicity Z (Fig. 1). At Z<0.01 this ratio rises much faster than current Galactic evolution models [9] predict and suggest an early source of the heavy Si isotopes not considered in these models, which are mainly based on Type II supernova nucleosynthesis.

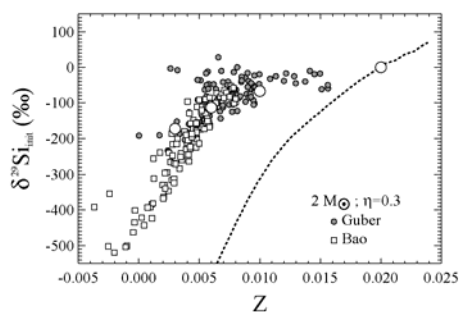


Figure 1. Predicted evolution of <sup>29</sup>Si/<sup>28</sup>Si as function of metallicity based on Z grains and the FRANEC models of a 2M<sub>⊙</sub> star with Reimers mass loss η of 0.3 and two sets of Si cross sections. This evolution is compared with the GCE model of Timmes and Clayton [9] (dotted line). The large open circles are the ratios assumed in our theoretical models.

References: [1] Nittler L. R. and Alexander C. M. O'D. 2003. *GCA* 67, 4961. [2] Bao Z. Y. et al. 2000. *Nucl. Data Tables* 76, 70. [3] Guber K. H. et al. 2003. *Phys. Rev. C* 67, 062802-1. [4] Hoppe P. and Ott U. 1997. In *Astrophysical Implications of the Laboratory Study of Presolar Materials*, (T. J. Bernatowicz and E. Zinner, eds.) 27. AIP, New York. [5] Hoppe P. et al. 1997. *ApJ*. 487, L101. [6] Amari S. et al. 2001. *ApJ*. 546, 248. [7] Nollett K. M. et al. 2003. *ApJ*. 582, 1036. [8] Jadhav M. et al. 2006. *New Astron. Rev.* in press. [9] Timmes F. X. and Clayton D. D. 1996. *Astrophys. J.* 472, 723.

**Fe-ISOTOPIC FRACTIONATION IN CB CHONDRITES.**

J. Zipfel<sup>1</sup> and S. Weyer<sup>2</sup>. <sup>1</sup>Senckenberg Forschungsinstitut und Naturmuseum, Senckenberganlage 25, 60325 Frankfurt am Main, Germany, jzipfel@senckenberg.de, <sup>2</sup>Institut für Mineralogie, J. W. Goethe-Universität Frankfurt, Germany.

**Introduction:** CB group meteorites share many properties with carbonaceous chondrites, such as presence of refractory inclusions, chondrules or chondrule fragments, high and unfractionated refractory element abundances. Yet some of their properties are unusual: extremely high FeNi-metal abundances, absence of hydrated matrix, and extreme depletions of moderately volatile lithophile and siderophile elements. In addition, chondrules in CB chondrites are ca. 5 m.y. younger than Calcium-Aluminum-rich Inclusions (CAIs) in CV3 chondrites [1, 2], and CAIs and chondrules don't show any evidence for the existence of live <sup>26</sup>Al at time of formation [3]. However, <sup>53</sup>Mn-<sup>53</sup>Cr systematics of HaH 237 follows the general trend defined by CI, CM, CO and CV carbonaceous chondrites and plots on an isochrone of ~ 4568 m.y., which is interpreted to indicate a general event of moderately volatile element loss, e.g. of Mn, at the start of the solar system [4], [5]. The low <sup>53</sup>Cr/<sup>54</sup>Cr ratio in HaH 237 is inconsistent with volatile loss 5 m.y. later during a separate event, such as vaporization in a giant impact cloud [6].

Evidence for a condensation origin of metal in HaH 237 is provided by chemically zoned metals with fractionated Fe isotopes. In these metals lighter Fe is concentrated in Ni-rich cores and heavier Fe in Ni-poor rims [7]. Iron isotopes of metal-rich "bulk samples" of HaH 237 and Isheyevo which both contain zoned metal grains [6] plot on a mass dependent fractionation line. Isheyevo contains the lightest Fe ( $\delta^{56}\text{Fe} = -0.443\text{‰}$ ) and HaH 237 slightly heavier Fe ( $\delta^{56}\text{Fe} = -0.297\text{‰}$ ), indicating that the fraction of light Fe which is probably sited in metal, is slightly higher in Isheyevo. Gujba does not contain any chemically zoned metal and a large metal aggregate separate that was analyzed has normal Fe isotope composition ( $\delta^{56}\text{Fe} = 0.025\text{‰}$ ) [6]. We have analyzed additional metal and silicate separates of the same meteorites plus samples from Bencubbin. The Fe composition of a second metal-rich Isheyevo sample is identical to our earlier findings. Preliminary data of silicates in Isheyevo have heavier Fe ( $\delta^{56}\text{Fe} = -0.032\text{‰}$ ). A separate of Gujba enriched in fine-grained metal shows significantly lighter Fe compositions ( $\delta^{56}\text{Fe} = -0.363\text{‰}$ ) than the previously analyzed coarse metal aggregate. This Fe isotope composition is similar to that of the HaH 237 and Isheyevo samples and indicates that fine grained metal in Gujba, although being chemically unzoned, must be derived from a source with similar Fe isotope composition.

**References:** [1] Krot A. N. et al. 2005. *Nature* 436:989–992. [2] Kleine T. et al. 2005. *GCA* 69:5805-5818. [3] Gounelle M. 2006. Abstract #2014. 37th Lunar & Planetary Science Conference. [4] Shukolyukov A. and Lugmair G. W. 2001. *Meteoritics & Planetary Science* 36:A188-A189. [5] Palme H. 2001. *Phil. Trans. R. Soc. Lond. A* 359:2061-2075. [6] Zipfel J. and Weyer S. 2006. #1902. 37th Lunar & Planetary Science Conference. [7] Alexander C. M. O'D. and Hewins R. H. 2004. *Meteoritics & Planetary Science* 39:A13.